A THESIS FOR THE DEGREE OF MASTER OF SCIENCE

Fabrication and Characterization of Flame-Retardant Nanocomposites based on Ethylene Vinyl Acetate and Cationic Clay

에틸렌 비닐 아세테이트 및 양이온성 클레이를 기반으로 한 난연 나노복합체의 제조 및 특성

By Jung-Hun Lee

PROGRAM IN ENVIRONMENTAL MATERIALS SCIENCE
GRADUATE SCHOOL
SEOUL NATIONAL UNIVERSITY
FEBRUARY, 2014

A THESIS FOR THE DEGREE OF MASTER OF SCIENCE

Fabrication and Characterization of Flame-Retardant Nanocomposites based on Ethylene Vinyl Acetate and Cationic Clay

에틸렌 비닐 아세테이트 및 양이온성 클레이를 기반으로 한 난연 나노복합체의 제조 및 특성

By Jung-Hun Lee

Advisor : Hyun-Joong Kim

PROGRAM IN ENVIRONMENTAL MATERIALS SCIENCE
GRADUATE SCHOOL
SEOUL NATIONAL UNIVERSITY
FEBRUARY, 2014

Fabrication and Characterization of Flame-Retardant Nanocomposites based on Ethylene Vinyl Acetate and Cationic Clay

에틸렌 비닐 아세테이트/양이온성 클레이를 기반으로 한
난연 나노복합재료의 제조 및 특성

지도교수: 김 현 중

이 논문을 농학석사학위 논문으로 제출함
2013 년 12 월

서울대학교 대학원
산림과학부 환경재료과학전공
이 정 훈

이정훈의 석사학위 논문을 인준함
2013 년 12 월

위 원 장 최 인 규 (인)

부위원장 김 현 중 (인)

위 원 최 준 원 (인)

Abstract

Fabrication and Characterization of Flame-Retardant Nanocomposites based on Ethylene Vinyl Acetate and Cationic Clay

Jung-Hun Lee
Program in Environmental Materials Science
The graduate School
Seoul National University

Polymer/layered silicate (PLS) nanocomposites have attracted great interest, because they have shown remarkable effects in mechanical properties, thermal stability and flame retardants. The main objective of this study is to investigate the effect of particle size and organic modifier of clay in ethylene-vinyl acetate/clay composites. First, different particle sized pristine smectite clays, S1ME and Laponite-XLG, were selected and the pristine clays were modified with two different akyl ammonium surfactants. Ethylene-vinyl acetate (EVA)/pristine clay or organoclay masterbatches were prepared with solution blending to prevent the loss of clay and to introduce the well dispersion. Nanocomposites were compounded via melt blending with the masterbatches and maleic anhydride grafted EVA (MA-g-EVA) as compatablizing agent.

In addition, the optimum organoclay for mechanical properties and flame retardants was selected and determined of various concentrations. The nanocomposites were characterized using FT-IR spectroscopy to

determine the organic modification. Modification effect on the dispersion was investigated by using X-ray diffraction (XRD) and scanning electron microscopy (SEM). Universal testing machine (UTM) and dynamic mechanical analysis (DMA) were used to study tensile properties and dynamic mechanical property of the nanocomposites. To investigate the thermal degradation, thermogravimetric analysis (TGA) was employed. The final nanocomposites were characterized in terms of flame retardant properties by cone calorimeter.

Keywords : Polymer/layered silicate nanocomposites, Smectite clay, Organoclay, Ethylene-vinyl acetate, Mechanical properties, Flame retardants

Student Number : 2012-21119

CONTENTS

Chapter 1

Introduction, Literature reviews and Objectives

Chapter 2

Fabrication and Characterization of Nanocomposites with different Particle Size Cationic Clays and Organic Surfactants

Chapter 3

Further Study

List of Tables

List of Figures

Chapter 1

Introduction,

Literature Reviews and

Objectives

1. Introduction

1.1. Background of this study

In recent years, polymer/layered silicate (PLS) nanocomposites have attracted great interests, both in industry and in academia, because they often exhibit remarkable improvement in properties of materials when compared with pristine polymer of conventional micro- and macro-composites (Sinha Ray and Okamoto, 2003). And the aim to obtain fine composites is weight lightening and this can be produced by adding just a little amount of clay to a polymer matrix. For example, the addition of 2-5 wt. % of clay fillers doubles the tensile strength and the modulus, triples the heat distortion temperature, and reduces the gas permeability by a factor of 2 (Ginzburg *et al.*, 2000). Owing to strong interactions between the layered silicate particle and the polymer matrix, decreased interparticle distances and geometrical anisotropy of platelets, significant morphological changes occur. This leads to improvements in the permeation-barrier thermal stability and flame retardency (Osman *et al.*, 2005).

Ethylene vinyl acetate (EVA) is used widely in electrical insulation, cable

For the optimal performance of nanocomposites, the clay fillers are uniformly dispersed in the polymer matrix. So, there has been considerable interest in how to disperse the layer of silicate clay mineral more effectively in organic/inorganic polar polymer. Organic modification of layered silicates is commonly performed to render the inorganic clay platelets more organophilic to facilitate their incorporation in to a polymer matrix (Pavlacky and Webster, 2012).

This study is focused on analyzing effect of particle size of clay and two different organic modifiers to ethylene-vinyl acetate

(EVA)/smectite clay nanocomposites in mechanical, thermal and barrier properties.

1.2. Ethylene vinyl acetate (EVA)

Ethylene vinyl acetate (EVA) is the copolymer of ethylene and vinyl acetate. EVA is widely used in the wire, cable, wrapper, adhesive and drug industry (Wang *et al.*, 2012). The low cost and comparatively good electrical and barrier properties of EVA have led to the continuous increase of attention for market. As shown in Figure 1, the properties of EVA are determined by their vinyl acetate (VA) contents and their melt index (MI). MI signifies the melt flow property of polymer at particular pressure and temperature. The domain structure of EVA consists of stiff and partially crystalline polyethylene blocks, and flexible, soft and polar amorphous vinyl acetate blocks (Park *et al.*, 2006). Since, EVA is able to have a diversity of properties depending on the VA content in the copolymer, various EVA with different properties are easily supplied from market. However, the low tensile strength, thermal stability of EVA has limited its applications in some fields (Hoang *et al.*, 2013, Wang *et al.*, 2012).

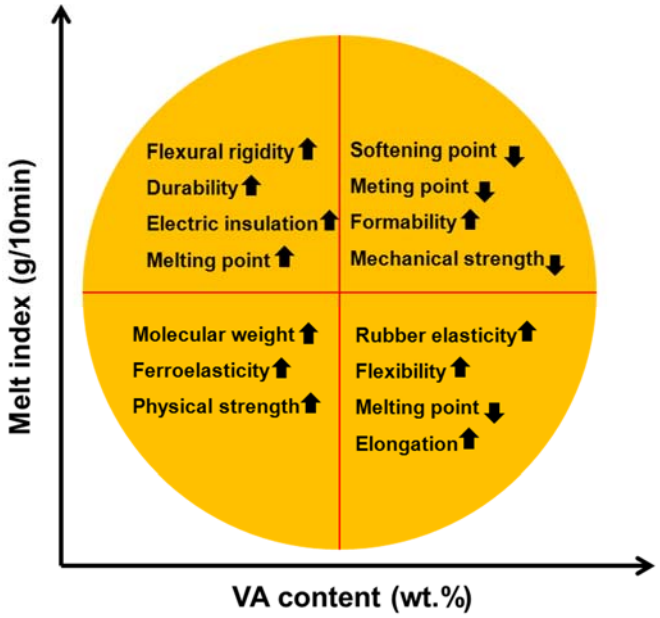

Figure 1. Grade selector chart for ethylene vinyl acetate (EVA) (www.solarnenergy.com)

1.3. Smectite clay

In the past few years, there has been increasing interest in smectite clay. Although this clay is hydrophilic nature, it has high cation exchange capacity, swelling capacity, high surface area, and resulting strong adsorption/absorption capacities (Xi *et al.*, 2004). So, chemical modification of smectite clay is easy and necessary in order to utilize their high internal surface area efficiently (Michot and Pinnavaia, 1991).

Among the commercialized clays, trioctahedral smectite such as sodium fluorine mica (S1ME, Co-Op Chemical Co., Ltd.) and laponite (Laponite XLG, Rockwood Additives Ltd.) are most common. As shown in Figure 2, they have two tetrahedral sheets sandwiching an octahedral sheet. Owing to exist isomorphic substitution within the layers (for example, Al^{3+} replaced by Mg^{2+} or Fe^{2+} in the octahedral sheet and Si^{4+} replaced by Al^{3+} in the tetrahedral sheet), the clay layers have negative charges and are counterbalanced by exchangeable cations such as Na^{+} and Ca^{2+} in the interlayer. Because of the hydration of inorganic cations on the exchange sites, the clay has hydrophilic surface that is immiscible with organic polymer. Thus, the surface treatment via ion exchange of the inorganic cations with organic cations is necessary.

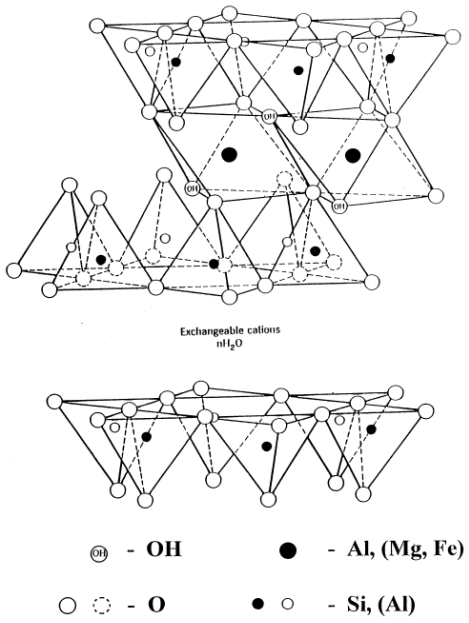

Figure 2. Structure of 2:1 layer of smectites (Madejova´ *et al.*, 1998)

1.3.1. Organic modified clay (Organoclay)

To obtain fine miscibility between clay and polymer, layered silicates should be either intercalated or exfoliated. In general, intercalation and exfoliation are observed when a polymer matrix and layered silicates have strong attractive reaction. Thus, the most important thing in the preparation of nanocomposites is how to provide strong attractive interactions between them (Lee and Han, 2003b). However, layered silicates have hydrophilic surface that interrupt interaction between filler and matrix. Therefore, it is essential to chemically modify a natural clay, such that it can become compatible with a polymer (Lee and Han, 2003a).

In this step, quaternary ammonium compounds usually have been used for enhance the surface properties. As you shown in Figure 3, the intercalation of a cationic surfactant not only changes the surface properties from hydrophilic to hydrophobic but also greatly increases the basal spacing of the layers (Boyd *et al.*, 1988).

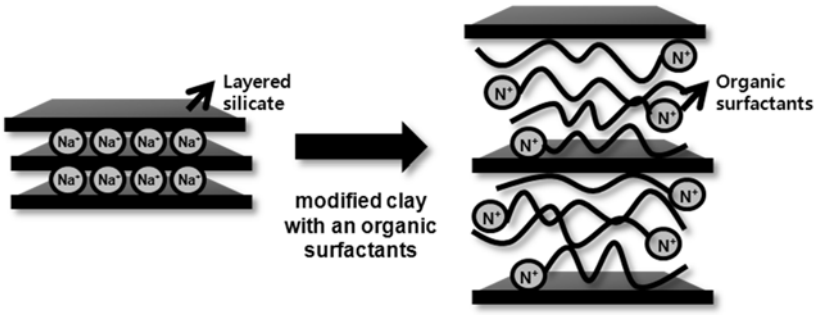

Figure 3. Scheme of organic modification of clay (Xi *et al.*, 2004)

1.4. Compatibilizing agent

In the past two decades, inorganic fillers, carbon black, silica, calcium carbonate (CC) and talc are used in composites. Among such these fillers, CC and talc are the most widely used thermoplastic in the plastic industry. But, these days organic fillers have become a strong competitor to inorganic fillers due to their low densities, very low cost, non-abrasiveness, recyclability, biodegradability and renewable nature (Premalal *et al.*, 2002). Due to a lack of resources and increasing environmental pollution, many researchers on the development of composites prepared using agro-wastes or lignocellulosic materials as reinforcing fillers. Since composites prepared using natural reinforcing fillers are inexpensive and could minimize environmental pollution due to their characteristic biodegradability, they could function as a method in solving the environmental problems that we would otherwise have to face in the future (Yang *et al.*, 2007).

In spite of these various forceful properties, the poor interfacial adhesion between the fiber and the matrix is a major problem that contributes unfavorable mechanical properties of composites. This is due to the difference in polarity between the hydrophobic polymer and the hydrophilic natural fiber (Khan and Bhattacharia, 2007, Thirmizir *et al.*, 2011). The most reliable means for improving interfacial adhesion between fiber and matrix is the introduction of a compatibilizing agent that contains functional groups, which can help out the surface of fiber and the polymer phase. Maleated polyolefins, such as maleated polypropylene and maleated polyethylene, are commercially used in the composite industry (Keener *et al.*, 2004).

1.4.1. Maleic anhydride grafted polymer (MA-g-polymer)

In the process for polymer/layered silicate nanocomposites, both in situ polymerization and intercalation from solution have limitation because neither a suitable monomer nor a compatible polymer-silicate solvent system is always available. These disadvantages drive the researcher to the direct melt intercalation method, which is the most versatile and environmental friendly method of preparing polymer/layered silicate nanocomposites (Pavlidoua and Papaspyridesb, 2008).

The addition of filler to polymer is most often used to improve the mechanical properties of the thermoplastics. In process of fabrication, the incompatibility between a polar filler and nonpolar polymer matrix caused poor dispersion of the filler in the matrix. To surmount this obstacle, a compatibilizing agent is usually added (Dikobe and Luyt, 2010). The direct polymer melt intercalation method is the simplest but there is still constraint caused from the hydrophilic silicate (Porter *et al.*, 2000). Thus, a functional group must be introduced to intercalate polymer with no polar group between the clay layers as Figure 4 (Hasegawa *et al.*, 2000).

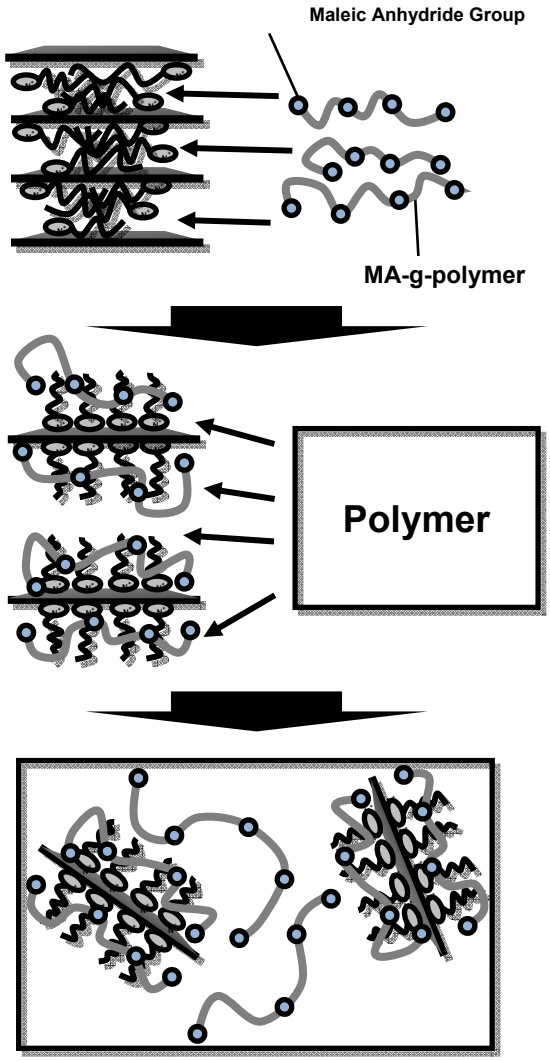

Figure 4. Scheme of polymer intercalation in the silicates in the presence of MA-g-polymer (Mittal, 2009)

1.5. Predispersion

Degree of dispersion is the most important factor to enhance nanocomposites properties. And as mentioned above, melt processing is obviously beneficial compared to solvent process because it is environmentally friendly (does not require handling dangerous solvents often associated with high performance polymers), involves significantly shorter cycle times, is easier to process, is often economically more attractive and makes some large scale applications feasible (Naffakh *et al.*, 2010). Although the organic modified clay layer surface is covered by the organic modifier, it still has some degree of hydrophilic property which has been proved by the preference of the organic clay to the polyamide 6 phase when the organic clay was blended with polystyrene and polyamide 6 *(Yang et al., 2008)*. In this reason, it has limit to disperse layered silicate in matrix homogeneously. Therefore, organoclay is predispersed in polymer as a masterbatch which used in melt processing. The introduction of the masterbatch (MB) in the corresponding polymer melt resulted in nanocomposites, whereas direct melt blending of the components in microcomposites (Siengchin and Karger-Kocsis, 2009).

1.6. Cone calorimeter

The cone calorimeter test is the most significant of small scale instruments in flame retardant. Heat release rate (HRR) is the most important parameter for characterizing an unwanted fire (Figure 5a). Over the test period, the peak heat release rate (pkHRR) is the maximum heat release rate which can be main factor of fire hazard. Average heat release emission (AHRE) is also another great parameter to determine flame retardants (Figure 5b). It is defined as the cumulative heat emission divided by time. The maximum average release emission (MAHRE), from this data, has been proposed as a good measure of the propensity for fire development under real scale conditions (Duggan *et al.*, 2004).

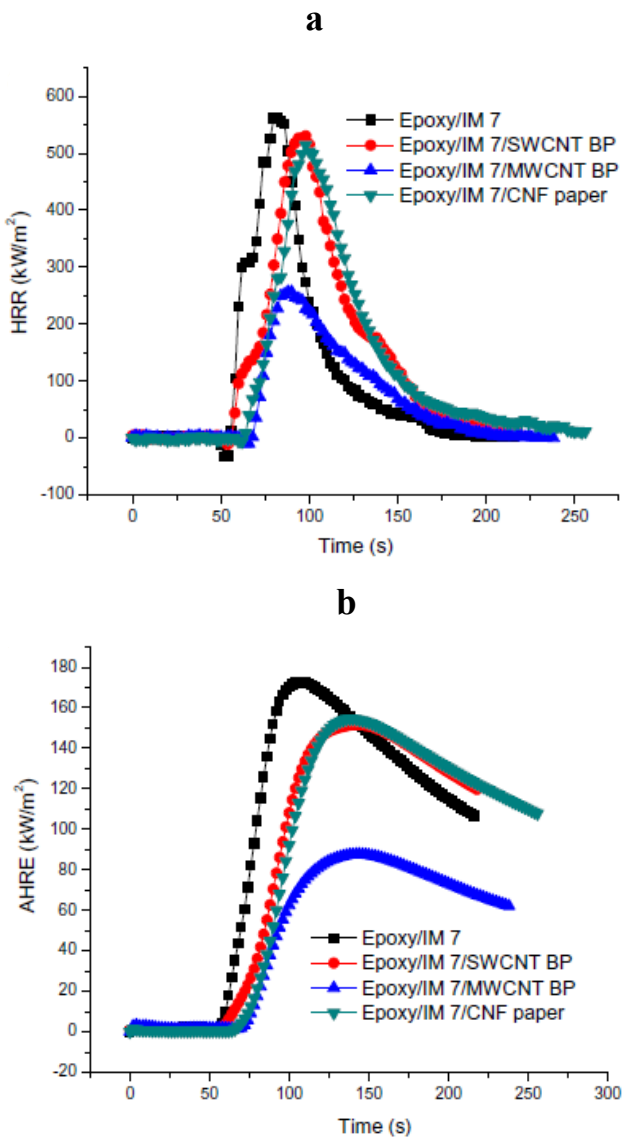

Figure 5. Examples of heat release rate (HRR) and average heat release emission (AHRE) of nanocomposites (Wu *et al.*, 2010)

2. Literature reviews

2.1. Nanocomposites composed of ethylene vinyl acetate (EVA)

Alexandre, M *et al.* (Alexandre *et al.*, 2001) prepared nanocomposites based on EVA and montmorillonite modified by various alkylammonium cations were obtained by melt intercalation. The Young's modulus of the obtained nanocomposites was significantly increased by the addition of 5 wt. % of nanofiller. Interestingly, when degraded under air (thermooxidation) the materials exhibited large improvement in the thermal stability by 40 K. EVA based nanocomposites showed interesting flame retardant properties such as reduction (by 47 %) for the peak of heat release.

Riva, A *et al.* (Riva *et al.*, 2002) fabricated the composites which based different modified fillosilicates and EVA polymer were mixed at 120 ^{o}C by melt compounding. The composites were showed the different structures of the particle dimensions (micro, intercalated and exfoliated nanocomposites). The effect of the composites structure on material rheological behaviour, is a dramatic increase of the storage and loss modulus in the nanocomposites, compared with the no filled polymer and with the microcomposites. The properties of nanocomposites were depending on the dispersion of the inorganic phase.

2.2. Introduction of compatibilizing agent in melt blending

Hoang, T *et al.* (Hoang *et al.*, 2013) reported fabrication of nanocomposites containing 2 to 5 wt.% silica nanoparticles (SNP) and 0 to 2 wt.% MA-g-EVA were prepared by the melt mixing of EVA and SNP. The use of MA-g-EVA produced remarkable enhancement in the relative melt viscosity, tensile strength, elongation at break, thermal stability and weatherability of the EVA/SNP nanocomposites. In particular, the weatherability of the EVA/SNP nanocomposites was clearly improved using only 1~1.5 wt.% of MA-g-EVA and 3 wt.% of SNP.

Suh, I *et al.* (Suh *et al.*, 2004) fabricated various vinyl acetate contents of ethylene vinyl acetate copolymer based montmorillonite (MMT) nanocomposites using melt blending. The effects of vinyl acetate content and concentration of grafted maleic anhydride in maleic anhydride grafted polyethylene (PEMA) were investigated. Improvement of dispersibility of MMT under the addition of PEMA was observed with increasing vinyl acetate content and it was attributed to the synergic effect of polar groups, i.e., vinyl acetate and maleic anhydride.

2.3. Effect of predispersion in nanocomposites

Yang, J *et al.* (Yang *et al.*, 2009) prepared a series of polystyrene (PS)-clay nanocomposites based on the different clays and the different predispersion methods prepared via in situ emulsion polymerization. The results from X-ray diffraction and TEM distinctly indicate that the types of clay and the predispersion methods have a significant influence to the microstructure of the nanocomposites. These results influenced storage modulus which had different enhancement over that of the pure polymer, when the temperature approaches the polymer's T_g.

3. Objectives

The main objective of this research was to prepare the nanocomposites composed of EVA, clays and MA-g-EVA with enhancement in the mechanical properties, thermal degradation behavior and fire retardant propensity. However, it is difficult to get well dispersed nanocomposites because clay has high internal surface energy and hence it has a tendency to agglomerate. This inclination is an obstruction to the properties of nanocompoistes.

In order to improve dispersion of clays in nanocomposites, three methods were introduced in this study. First, different particle size of pristine clays were modified with two kinds of organic surfactants. Second, EVA/clay solution (ECS) series were prepared to get the predispersion and to prevent the loss of clays in melt blending. Third, MA-g-EVA was introduced EVA/ECS series in melt blending. MA as functional groups can be intercalated between the silicate layers. Also, the proper amount of organoclay for nanocomposites' properties after the most suitable clay was selected.

Introduction of organic surfactant into silicate layers, it would be expected to improve the mechanical properties, thermal degradation and flame retardant. So, this research was focused on the influence of clay particle size, organic surfactants and to determine the optimum concentration of suitable clay on the mechanical properties, thermal degradation and flammability.

Chapter 2

Fabrication and Characterization of Nanocomposites with different Particle Size Clays and Organic Surfactants

1. Introduction

During the last two decades, researches focused on polymer nanocomposites (PNCs) with good practical properties have roused more attentions from many countries and regions. Due to the large surface-to-volume ratio between the nanoparticles and the polymer, considerable properties can be changed for relatively low concentrations of particles (Chao and Riggleman, 2013).

However, aggregation of the nanoparticles has a bad influence on the composites. Organic modification of nanoparticle is very important for inorganic nanoparticles to get well dispersion. Because introduction of organic surfactant lead to their sorption capacity towards the hydrophobic polymer, thus improving their sorption capacities are of great important (Zhu *et al.*, 2011).

Also, the effects of particle size of fillers were studied for long times. Linear low density polyethylene (LLDPE) were used to prepare composites with micron sized (mZnO), submicron sized (sZnO), and nanosized (nZnO) powders and investigated on mechanical properties, electrical and thermal conductivities of the composites (Ozmihci and Balkose, 2013). Mechanical and thermal properties of graphite oxide (GO)-phenolic composites were evaluated for different sizes (4, 40, and 140, μm) of GO. The composites exhibited better mechanical properties with larger sizes of GO particles.

In this study, different particle sizes of clays and two kinds of organic surfactants were used to investigate the effect on mechanical properties, thermal degradation and flame retardants.

2. Experimental

2.1. Materials

The EVA (VS420) with 21.5 wt.% vinyl acetate (VA) content supplied by LOTTE CHEMICAL, Republic of Korea, had a density of 0.945 g/cm^3, a melting point of 79 ˚C, melt flow index of 2.0 g/10 min. Maleic anhydride grafted ethylene vinyl acetate (MA-g-EVA) supplied by Du Pont, had a density of 0.91 g/cm^3, a melting point of 71 ˚C, and a melt flow index of 1.4 g/10 min. The layered silicates used in this study were S1ME (Na-fluorine) from Co-Op Chemical Co., Ltd, Japan and Laponite XLG (Synthetic nanoclay) from Rockwood Additives Ltd. The former one had 101.7 mequiv./100 g of cationic exchange capacity, the d-spacing is 12.6 Å of *d*-spacing and the particle size is over ~1200 nm, the latter had 119 mequiv./100 g of cationic exchange capacity, the d-spacing is 13.5 Å of *d*-spacing and the particle size is over ~25 nm (Table 1). As shown in Figure 6, cetyltrimethylammonium bromide (Sigma-Aldrich Korea Ltd.) and benzyldimethylstearylammonium chloride (Tokyo Chemical Industry Co., Ltd.) were used as organic surfactants. Toluene was purchased from Samchun Chemical Company, Republic of Korea.

Table 1. Typical properties of clay

	Laponite-XLG (Lap)	S1ME (ME)
Structure	$Na_{0.7}[(Si_8Mg_{5.5}Li_{0.3})O_{20}(OH)_4]$	$Na_{0.7}(Mg_{2.65}Si_4)O_{10}F_2$
Cation exchange capacity (meq/100 g clay)	119	101.7
d001 (Å)	13.5	12.6
Particle size (nm)	~25	~1200

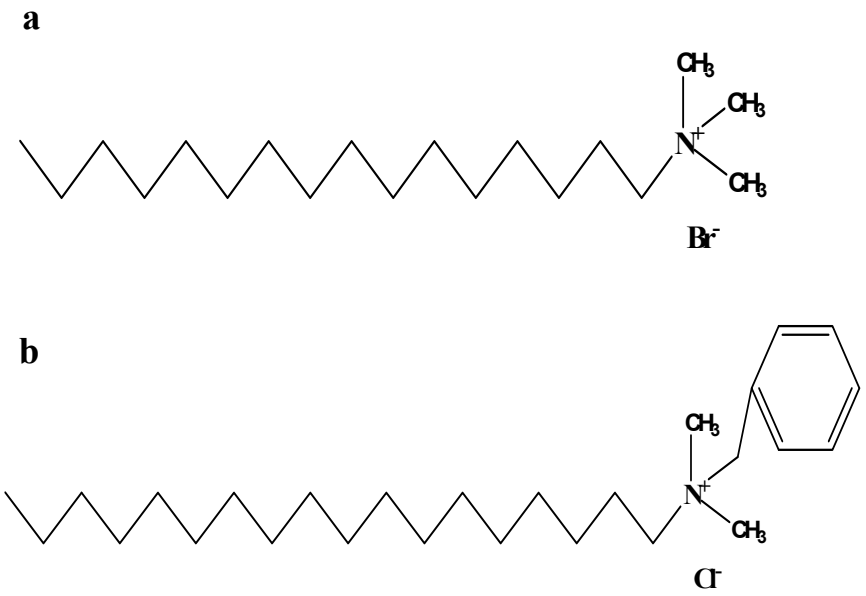

Figure 6. Chemical structure of organic surfactants:

(a) cetyltrimethylammonium bromide (CTAB),

(b) benzyldimethylstearylammonium chloride (BDAC)

2.2. Methods

2.2.1. Preparation of organoclays

The organoclays were synthesized as follows: 20 g of pristine clays were first swelling in 1000 mL of deionized water for 24 hours and then the alkylammonium surfactants were added slowly. The concentration of alkylammonium added is 1.0 cation-exchange capacity (CEC) of host clays. The reaction mixtures were stirred for 24 hours at 80 ˚C. The final reaction products were separated by centrifugation, freeze dried, ground and oven dried for 24 hours at 100 ˚C. The organoclays were named ME-CTAB, ME-BDAC, Lap-CTAB and Lap-BDAC depending on the clays and the alkylammonium surfactants.

2.2.2. Preparation of EVA/clay predispersions

First, the EVA was added to toluene under stirring at 90 ˚C for 1 hour. The dispersion of pristine clay and organoclay in the same solvent, prepared by stirring for 6 hours at 90 ˚C, was added to the EVA solution and then continuously stirred for 24 hours. A total of the solution was placed in a PET release film and evaporated in oven at 100 ˚C for 12 hours. Table 2 shows the blending ratio of predispersions.

Table 2. Blend ratio of EVA/clay predispersions

Samples	Clay (g)	EVA (g)
ECS-Lap	Lap (5)	20
ECS-Lap-CTAB	Lap-CTAB (5)	20
ECS-Lap-BDAC	Lap-BDAC (5)	20
ECS-ME	ME (5)	20
ECS-ME-CTAB	ME-CTAB (5)	20
ECS-ME-BDAC	ME-BDAC (5)	20

Lap (Laponite XLG, laponite)

ME (S1ME, mica),

CTAB (Cetyltrimethyl ammonium bromide)

BDAC (Benzyldimethylstearyl ammonium chloride),

ECS (EVA/clay solution, predispersion)

2.2.3. Compounding of EVA/ECS series/MA-g-EVA nanocomposites

EVA was dried at 60 ˚C for 24 hours and stored in polyethylene bags. EVA /ECS series were blended with the MA-g-EVA in a laboratory-sized, co-rotating, twin screw extruder (BA19, Bau Technology, Republic of Korea) using three general processes: melt blending, extrusion and pelletizing. The extruder barrel was divided into eight zones with the temperature in each zone being individually adjustable. The temperature of the mixing zone in the barrel was maintained at 100 ˚C with a screw speed of 300 rpm. The strand after extruding was cooled in a water bath and pelletized with pelletizer (Bau Technology, Republic of Korea). The final pellets were oven dried at 80 ˚C for 24 hours and stored in sealed polyethylene bags to avoid moisture permeation. Table 3 shows the blend ratio of nanocomposites compounded in this work. And Figure 7 shows the manufacturing process of melt blending.

Table 3. Blend ratio of EVA/ECS series/MA-g-EVA nanocomposites

Samples	ECS series (g)	EVA (wt.%)	MA-g-EVA (wt.%)
Pure EVA	0	100	0
ECM-Lap	ECS-Lap (25)	75	5
ECM-Lap-CTAB	ECS-Lap-CTAB (25)	75	5
ECM-Lap-BDAC	ECS-Lap-BDAC (25)	75	5
ECM-ME	ECS-ME (25)	75	5
ECM-ME-CTAB	ECS-ME-CTAB (25)	75	5
ECM-ME-BDAC	ECS-ME-BDAC (25)	75	5

ECM (EVA/clay melt blending, nanocomposites)

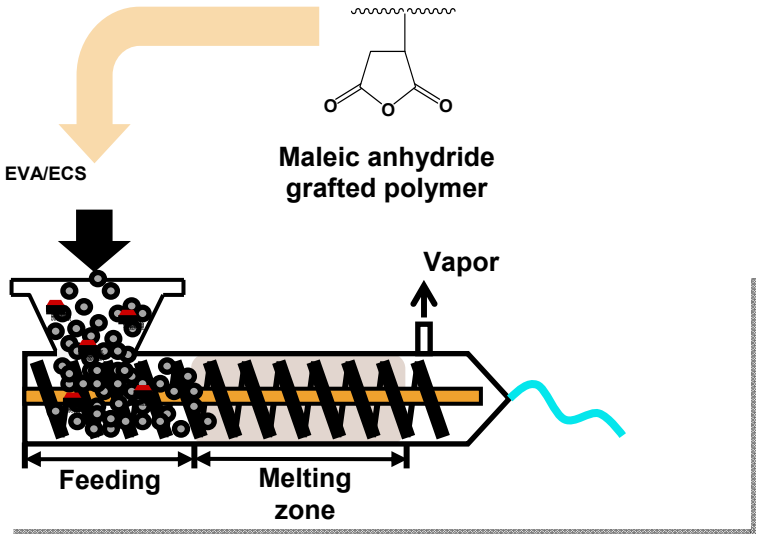

Figure 7. Manufacturing process of EVA/ECS series/MA-g-EVA nanocomposites

2.2.4. Injection molding

The dried extruded pellets were fabricated to specimens for tensile and DMA test through injection molding machine (Bau Technology, Republic of Korea). The conditions of temperature for injection molding were maintained at 100 ℃.

2.3. Characterization

2.3.1. Fourier transform infrared spectroscopy (FT-IR)

Pristine clays and organoclays were examined using a Fourier transform infrared (FT-IR) spectroscopy. The IR spectra were recorded using FT/IR-6100 (JASCO, Japan). The FT-IR spectra were collected over the range of 4000~500 cm^{-1} with a spectrum resolution of 4 cm^{-1}. All spectra were averaged over 30 scans.

2.3.2. X-ray diffraction (XRD)

X-ray diffraction analysis of pristine clay, organoclay powders and EVA/ECS/MA-g-EVA nanocomposites were performed using a Bruker X-ray diffractometer (equipped with a 2-D detector) in reflection mode. Tests were carried out with 2θ scanned between 2.0° and 10° nickel-filtered CuK$\propto$ radiation (k = 0.15418 nm) under a voltage of 40 kV and a current of 30 mA.

2.3.3. Cone calorimeter test

Flaming performance was characterized by cone calorimeter (Fire Testing Technology Ltd., UK) according to standard ISO 5660-1. Specimens (100 mm x 100 mm x 4 mm, W x L x T) were irradiated horizontally at a heat flux of 50 kW/m^2.

2.3.4. Tensile test

Tensile tests for the nanocomposites were carried out according to ASTM D 638-03 using a Universal Testing Machine (Zwick Co.) at a crosshead speed of 60 mm/min and a temperature of 23±2 ˚C. Seven measurements were done for each sample and final results were reported as averaged values.

2.3.5. Dynamic mechanical analysis (DMA)

The temperature dependence of the dynamic storage modulus (E') of nanocomposites were measured at a frequency of 1 Hz and at a strain rate 0.05 % at a heating rate of 2 °C/min over the temperature range of -40 °C to 40 °C. A dynamic mechanical analyzer (DMA Q800, TA Instruments) employing the dual cantilever method in rectangular specimens of 60.0 mm x 12.0 mm x 3.0 mm was used.

2.3.6. Scanning electron microscopy (SEM)

The morphology of the nanocomposites was examined using a scanning electron microscopy (SNE-3000M, Dream Corp., Republic of Korea). In order to get fractured surface, the SEM specimens were smashed after frozen with liquid nitrogen and were attached to aluminum stubs with a carbon tape. The specimen surfaces were then coated with gold to (purity, 99.99%) to eliminate electron charging.

2.3.7. Thermal gravimetric analysis (TGA)

TGA measurements were conducted with a thermo gravimetric analyzer (TGA 4000, PerkinElmer Inc., USA) on samples having masses from 5 to 7 mg. The heating rate was 10 ˚C/min over the temperature range from 60 to 600 ˚C; a nitrogen atmosphere was employed.

3. Results and Discussion

3.1. Fourier transform infrared spectroscopy (FT-IR)

To confirm organic modification in the silicate layers of organoclay and pristine clay as a reference were analyzed by FT-IR. Figures 8, 9, 10, and 11 show FT-IR spectra of the pristine clays, organic surfactants and organoclays. These results could be related with the organic modification between layered silicates and organic surfactants. And this is the comparable data for pristine clays and organoclays. For pristine clays, the band related to the stretching vibration of Si-O groups splits into a sharp band at around 1000 cm^{-1} (Figure 9). With the introduction of organic surfactants, no shift in the position of the main peak is observed. However, changes of the peak seem to depend on the type of intercalant structure (Souza *et al.*, 2011). For the organic surfactants and organoclays, the absorption peaks located at around 2920 cm^{-1} and 2850cm^{-1} can be assigned to the asymmetric and symmetric stretching C-H vibration respectively. The peaks allotted to the CH_2 scissoring from surfactants appeared between 1467 cm^{-1} and 1482 cm^{-1} and bands at around 1020 cm^{-1} for Si-O deformation from silicate layers. Overall, these peaks confirm that organic surfactants were efficiently introduced between silicate layers through cation exchange reaction. However, Figures 10 and 11 show peaks of CTAB series related with the alkyl tail of organic surfactants were higher than that of BDAC series. And there were no shift in IR spectra for different type of organic surfactants.

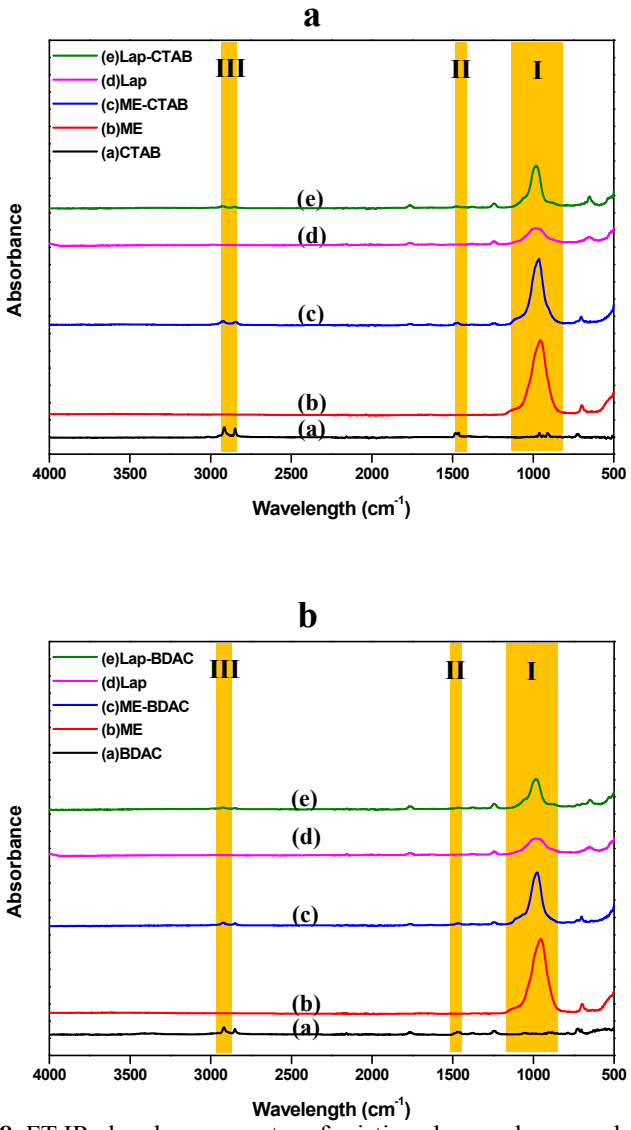

Figure 8. FT-IR absorbance spectra of pristine clays and organoclays:

(a) for CTAB, (b) for BDAC

The major bands in the range are shaded and will be shown in Figures 9, 10 and 11.

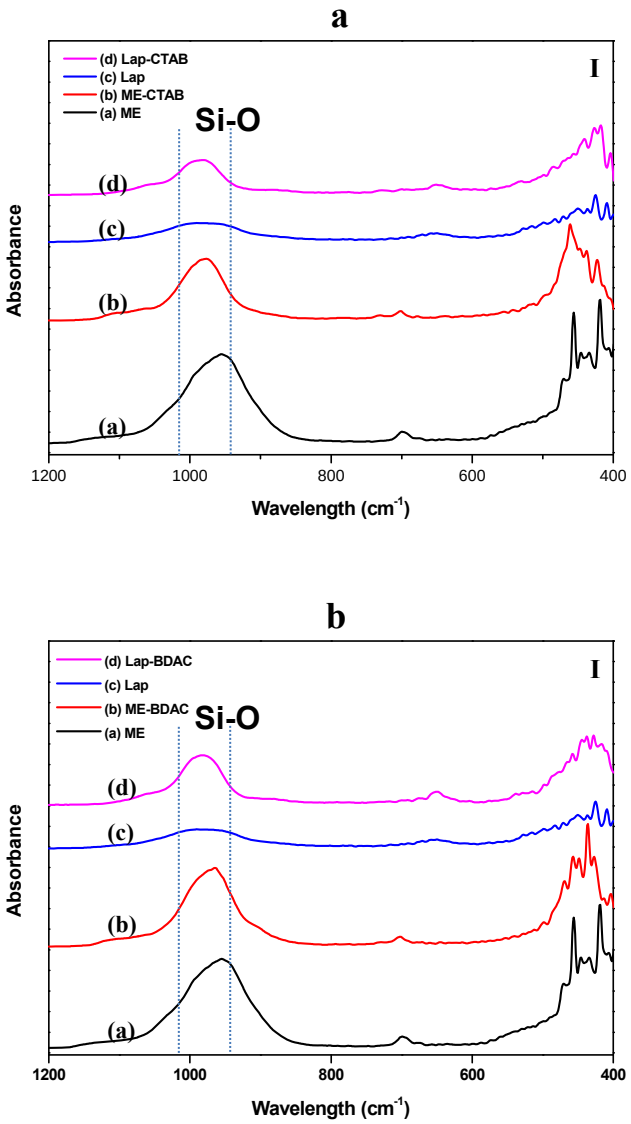

Figure 9. Major IR bands of pristine clays and organoclays from 1200 cm^{-1} to 400 cm^{-1}: (a) for CTAB, (b) for BDAC

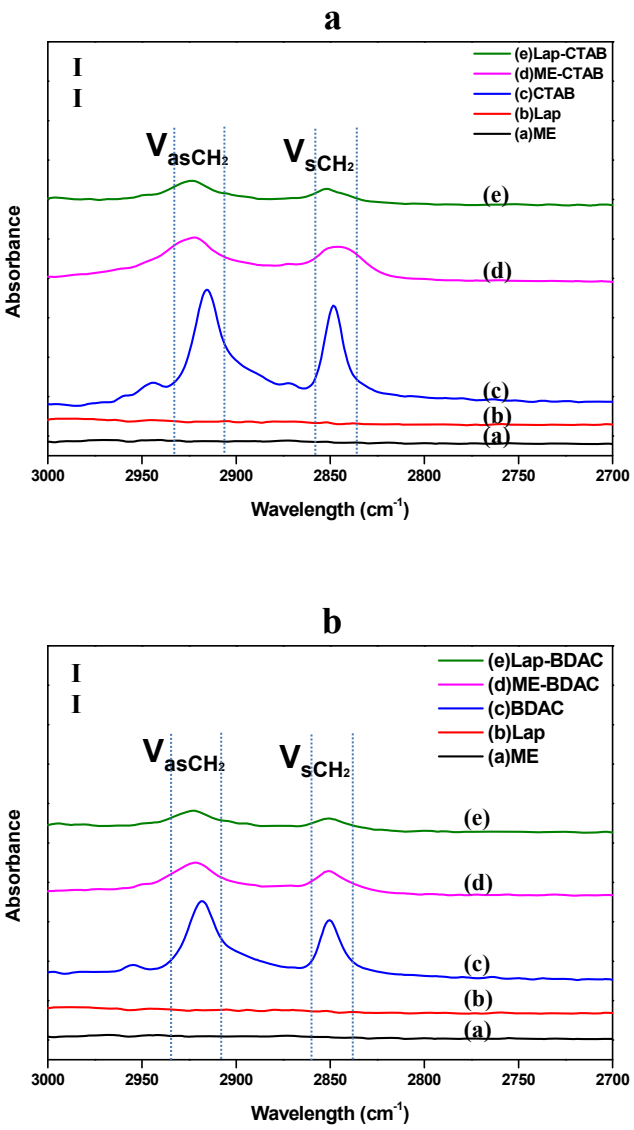

Figure 10. Major IR bands of pristine clays and organoclays from 3000 cm^{-1} to 2700 cm^{-1}: (a) for CTAB, (b) for BDAC

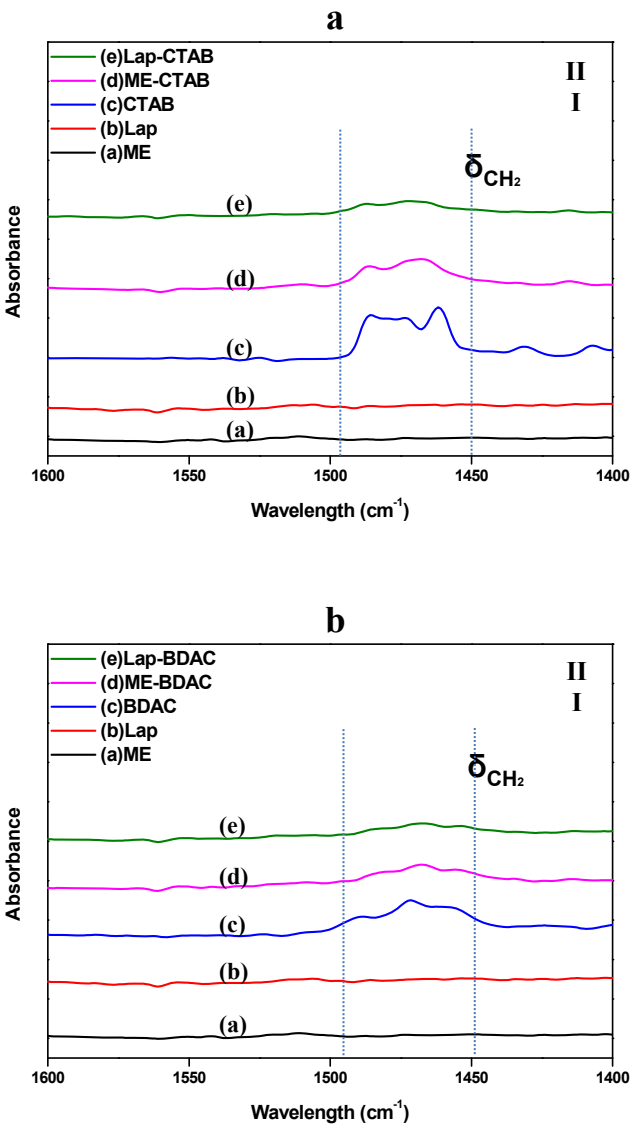

Figure 11. Major IR bands of pristine clays and organoclays from 1600 cm^{-1} to 1400 cm^{-1}: (a) for CTAB, (b) for BDAC

3.2. X-ray diffraction (XRD)

Figure 12 shows the evolution of XRD patterns for the organoclays synthesized based on different alkyl ammonium surfactants. The basal spacing (d_{001}) of pristine ME was 12.6 Å. In case of ME, the XRD pattern of ME-CTAB and ME-BDAC showed the reflection at 2θ = 2.14 (d = 41.3 Å) and 2θ = 3.64 (d = 24.3 Å) respectively, indicating that the intercalated alkylammonium cations were oriented parallel to the basal plane of the silicate layers (Yang *et al.*, 2001). On the other hand, pristine Lap had a 13.5 Å of the basal spacing which is higher than that of ME. However, Lap-CTAB and Lap-BDAC only had a peak at 14.7 Å and 18.0 Å respectively. From these data, it showed that lower particle size (~25 nm) can't make a big difference on basal spacing. It shows a similar tendency with FT-IR results. The benzene rings in quaternary ammonium have little impact on d-spacing of organoclay.

Figure 13 shows the XRD patterns provide useful information related to the variation in the basal spacing (d_{001}) of nanocomposites. The ME has basal space of 12.6 Å but, ECM-ME-CTAB and ECM-ME-BDAC have no peak due to the good dispersion of organoclay. These results can be explained that the exfoliated structures of the nanocomposites. In contrast, the XRD patterns for ECM-Lap series have a peak, indicating the intercalation of EVA into silicate layers. There is no complete exfoliation and exist of stacked silicate layers. As you see in Figure 12a, the peak was observed with introduction organic modified Lap representing worse dispersion than that of the nanocomposites with pristine Lap (Foungfung *et al.*, 2011, Limparyoon *et al.*, 2011). SEM results also support the agglomerated particle. These results will related with tensile modulus in the Chapter 3.4.

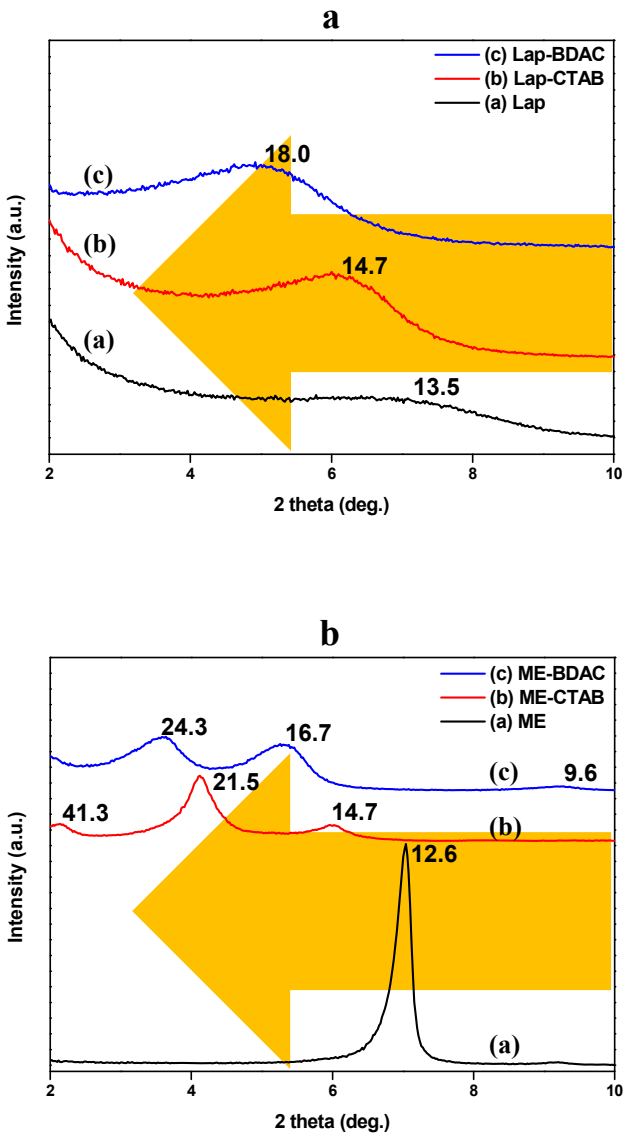

Figure 12. X-ray diffraction patterns of pristine clays and organoclays powder: (a) for Lap series, (b) for ME series

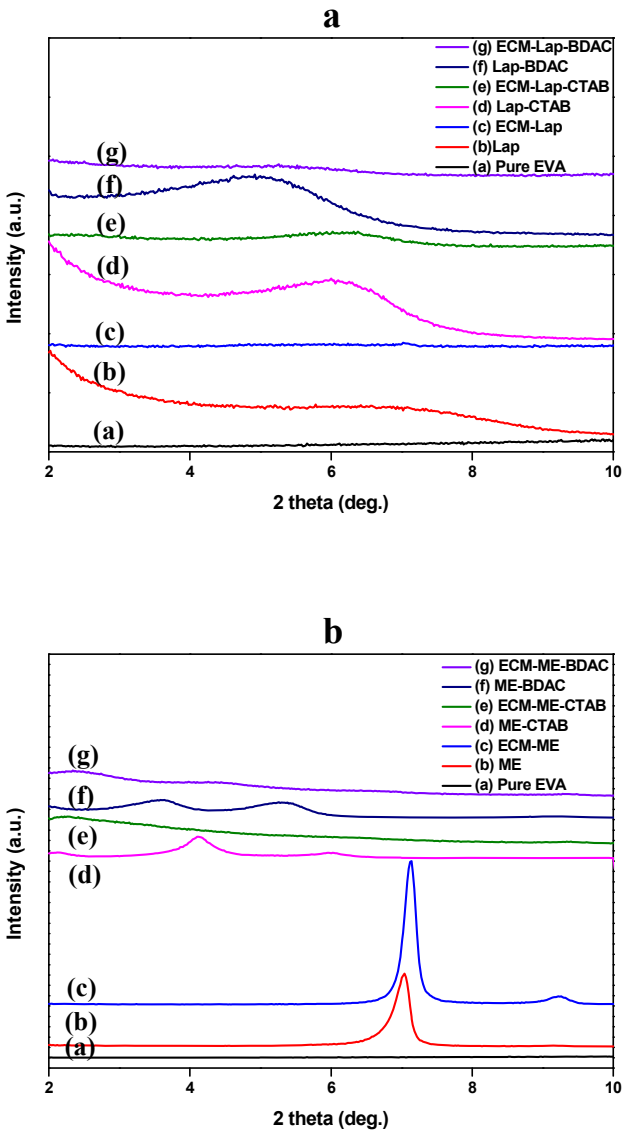

Figure 13. X-ray diffraction patterns of pure EVA and nanocomposites: (a) for Lap series, (b) for ME series

3.3. Cone calorimeter test

Cone calorimeter test is an effective method to measure the combustion behavior of nanocomposites. Valuable information on the combustion behavior was obtained from the test. The data from this test are important parameters and can be used to evaluate the propensity and developing of fires (Cao *et al.*, 2013).

Figure 14 reported the Heat Release Rate (HRR) curves of the studied samples. On disclosure to radiant heat, pure EVA became liquid, and then thermal degradation occurred. For about 340 s from the test beginning, the specimen generated volatile gases and there was no char. Also the nanocomposites displayed total heat release (THR) similar to that of pure EVA. This result can be explained there was no chemical reaction in fire (Table 4). Nanocomposites with ME showed broad curve, which corresponds to a fire risk decrease, compared with steep heat release rate in Lap. Compared between pristine ME and organic modified ME in combustion behaviors, pkHRR of nanocomposites with ME-CTAB showed slightly lower peak and broad curve.

Figure 15 reported the curve of the Average Heat Release Emission (AHRE), which is defined as the cumulative heat emission divided by time (Fina *et al.*, 2006) and its peak value (Maximum Average Heat Release Emission, MARHE) has been proposed as a good measure of the propensity for fire development under real scale conditions (Duggan *et al.*, 2004). In this research, MARHE for the ECM-ME-CTAB nanocomposites (428 kW/m^2) was 22% lower than that of the pure EVA (550 kW/m^2) (Monti and Camino, 2013). On the other hand, MARHE for the ECM-Lap series was higher than that of the pure EVA except Lap without organic modification. This tendency caused from agglomeration of clay due to high surface energy from its small particle size (~25 nm),

compared with ME (~1200 nm). After fire combustion, the char of ECM-ME series was more remarkable than that of ECM-Lap series (Figures 16 and 17). Even if the organic surfactants were applied to pristine clay, it can't derive the positive effect without well dispersion. In this case, introduction of organic surfactants was a causative factor in flame retardancy as in Figures 14a and 15a, pkHRR and MAHRE of ECM-Lap-CTAB and ECM-Lap-BDAC was higher than that of ECM-Lap.

From these data, nanocomposites with ME modified CTAB was the most efficient to minimize initial state fire accident. Although the organoclay is more miscible with organophilic polymer than pristine clay, it causes a little difference because of poor dispersion.

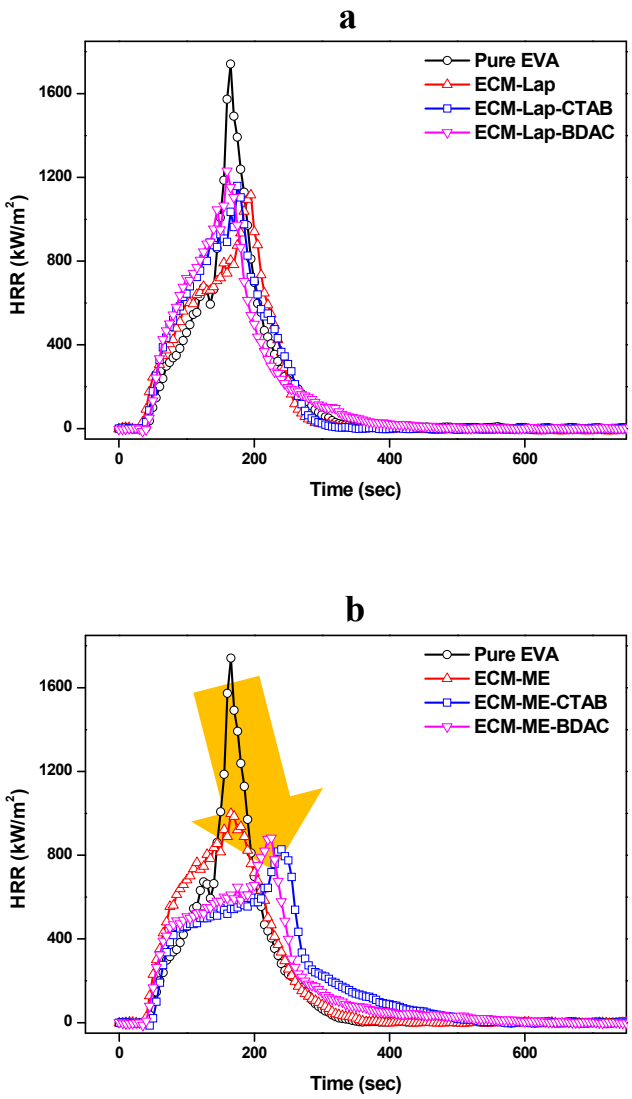

Figure 14. Heat release rate curves of the pure EVA and nanocomposites: (a) for Lap series, (b) for ME series

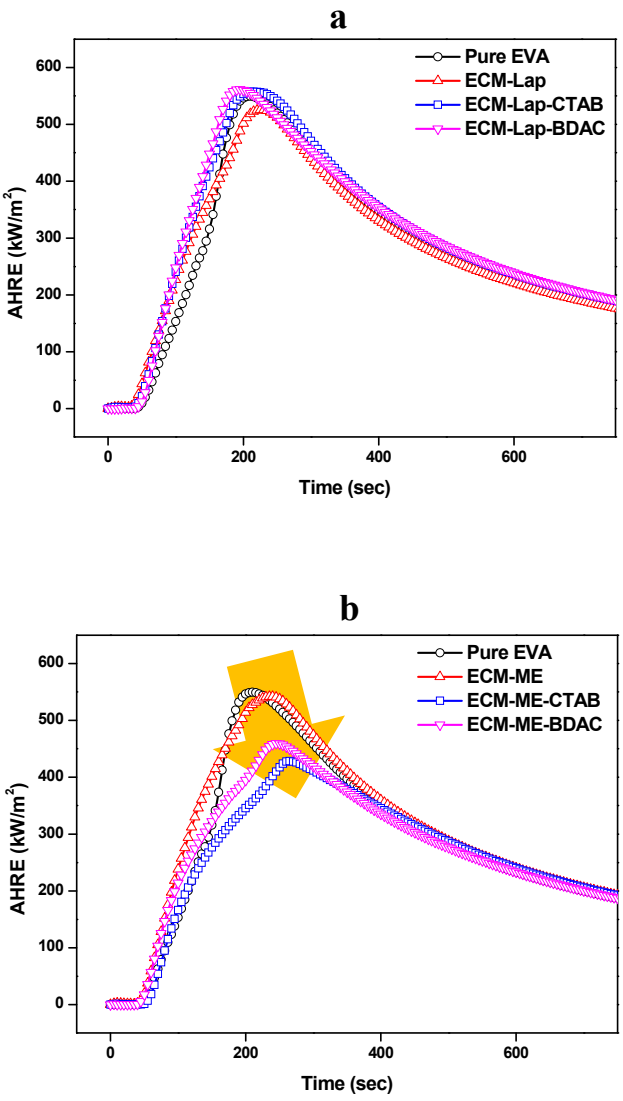

Figure 15. Average heat release emission curves of the pure EVA and nanocomposites: (a) for Lap series, (b) for ME series

Table 4. Cone calorimeter test results

Samples	Total heat release (MJ/m^2)	Peak of heat release rate (kW/m^2)	Maximum average heat release emission (kW/m^2)
	THR	pkHRR	MAHRE
Pure EVA	140.6	1740.8	549.6
ECM-Lap	132.4	1114.6	525.7
ECM-Lap-CTAB	142.1	1159.0	557.5
ECM-Lap-BDAC	144.3	1230.4	561.3
ECM-ME	144.0	951.6	542.0
ECM-ME-CTAB	144.1	827.1	428.5
ECM-ME-BDAC	140.7	883.2	459.5

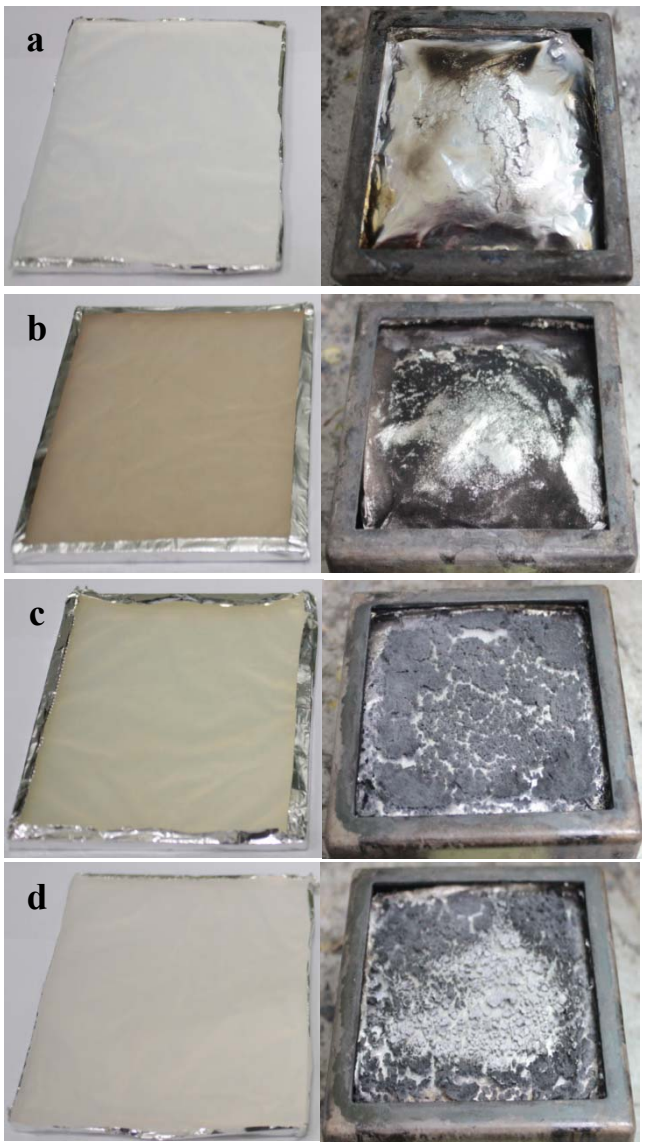

Figure 16. Mass residue after the cone calorimeter tests:
(a) pure EVA, (b) ECM-Lap, (c) ECM-Lap-CTAB,
(d) ECM-Lap-BDAC

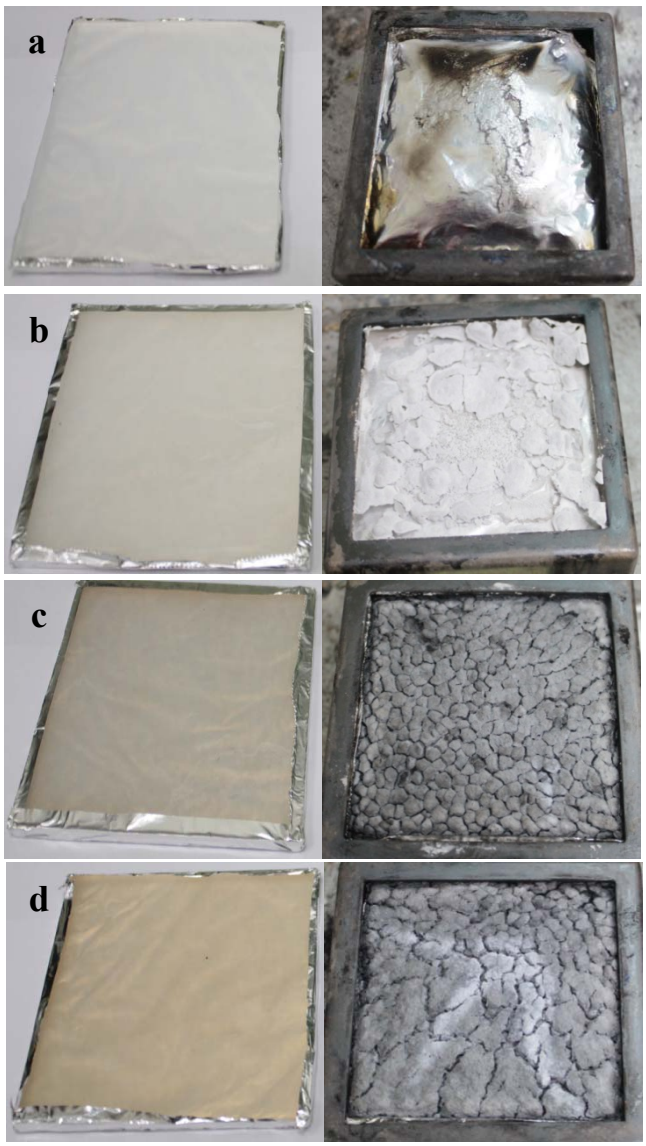

Figure 17. Mass residue after the cone calorimeter tests:
(a) pure EVA, (b) ECM-ME, (c) ECM-ME-CTAB,
(d) ECM-ME-BDAC

3.4. Tensile test

In this study, content of pristine clay and organoclay is fixed 5 phr to compare the influence of clay particle size in the same amount of fillers at first. With introduction of filler, the voids due to separation of the polymer from the filler caused from deformation generated and it is the main reason behind crack of nanocomposites (Bigg, 1987, Nugay and Erman, 2001). Also, agglomeration of clay lead to poor mechanical properties due to clay aggregation acts as impurities in nanocomposites (Asyadi *et al.*, 2013).

The variation of tensile properties for pure EVA and the nanocomposites are presented in Figure 18 and Table 5. Tensile strength of ECM-ME series is up around 3 ~ 11 % over that of pure EVA and EVA-ME-CTAB and EVA-ME-BDAC shows similar results higher than ECM-ME. ECM-Lap series reports that tensile strength is upgraded with the organic modification of pristine Lap, however, tensile strength of pure EVA is up around 6 ~ 15 % over that of ECM-Lap series. Table 5 shows tensile modulus of pure EVA and the nanocomposites. It seems to be similar trend with tensile strength and tensile modulus of ECM-ME series and ECM-Lap series is higher than that of pure EVA. But, as Lap series introduced in EVA, tensile modulus of nanocomposites decreased. The reason why this result occurred is agglomeration of clay due to Lap has so small particle size that it couldn't get fine dispersion.

At same load, clay with too small particle size couldn't do its role in nanocomposites. In addition, organic modification could have a helpful impact on the mechanical properties. As mentioned above, agglomeration of clay had a bad effect like impurities on mechanical properties of nanocomposites.

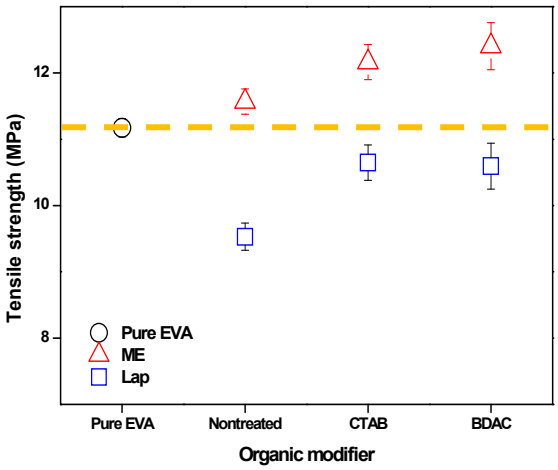

Figure 18. Tensile strength at break of pure EVA and nanocomposites

Table 5. Tensile modulus of pure EVA and nanocomposites

Sample	Tensile modulus (MPa)
Pure EVA	7.4
ECM-Lap	10.1
ECM-Lap-CTAB	9.4
ECM-Lap-BDAC	9.0
ECM-ME	9.5
ECM-ME-CTAB	12.1
ECM-ME-BDAC	13.6

3.5. Dynamic mechanical analysis (DMA)

The dynamic mechanical performances of pure EVA and nanocomposites were investigated by dynamic mechanical analysis (DMA). Two kinds of parameters were researched as a function of temperature. Figure 19 shows the temperature dependence of storage modulus (E') plots. The storage modulus of the nanocomposites with organoclays was higher than that with pristine clays. The data was improved by synergistic effect of the ME modified with CTAB. Table 6 shows the storage modulus of pure EVA and nanocomposites at 20 ˚C. In DMA test on EVA like rubber polymer, storage modulus has been investigated at 20 ˚C which can be expectation of modulus of nanocomposites. One possible explanation for these results, the EVA matric had slightly more restricted mobility due to the interaction with silicate layers. These behaviors might be associated with more effective in dispersion than pristine clays. However, ECM-Lap series were close to the value for pure EVA, which might be associated with the inhomogeneity of the intercalated structure of these nanocomposites (Shi *et al.*, 2007).

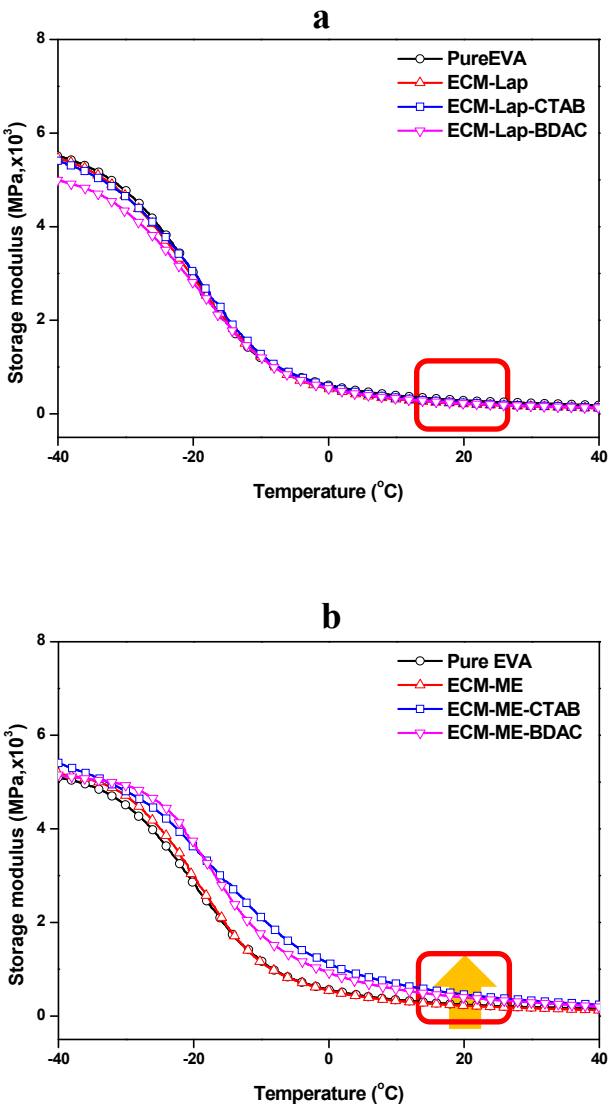

Figure 19. Storage modulus versus temperature plots:
(a) ECM-Lap series, (b) for ECM-ME series

Table 6. Storage modulus of pure EVA and nanocomposites

Sample	T_g (°C)	Storage modulus (E', MPa) at 20 °C
Pure EVA	-13.0	246.6
ECM-Lap	-11.1	213.0
ECM-Lap-CTAB	-11.7	238.0
ECM-Lap-BDAC	-11.5	224.1
ECM-ME	-12.5	224.7
ECM-ME-CTAB	-9.7	461.8
ECM-ME-BDAC	-12.3	398.7

3.6. Scanning electron microscopy (SEM)

The morphology of the nanocomposites was observed by scanning electron microscopy. Figure 20 shows the microstructure of EVA/clay/MA-g-EVA compound in different magnifications (x500, x2.0k). Pure EVA has no particle and fracture surface. The nanocomposites with pristine ME (ECM-ME) has agglomerative particles of size about 2~14 μm in diameter. On the other hands, the nanocomposites with organic modified clay (ECM-ME-CTAB and ECM-ME-BDAC) show no microscopic voids. This indicates that the layered silicates of nanocomposites do not agglomerate, and also this tendency of particles is an indication for the possibility to improve the properties of the final products (Akelah and Moet, 1996). However, the ECM-Lap series have completely different trend. In case of the series, they has flocculated particle. As this morphology can be explained the result that the modulus of ECM-Lap series from XRD and tensile test.

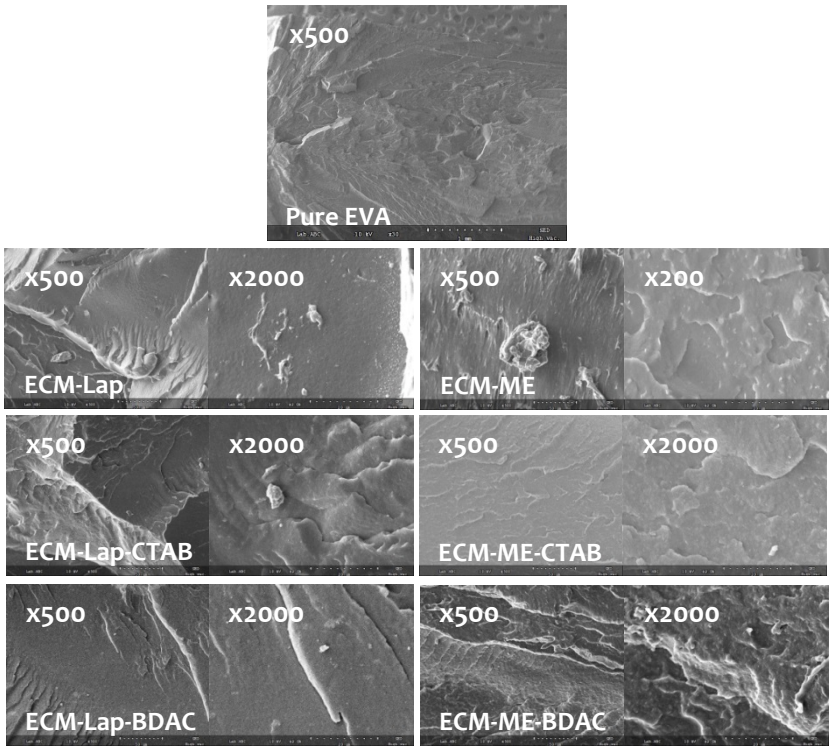

Figure 20. SEM images of Pure EVA and EVA/ECS series/MA-g-EVA nanocomposites

3.7. Thermal gravimetric analysis (TGA)

Figure 21 and Table 7 respectively show thermal gravimetric curves and data of pure EVA and nanocomposites with ME and Lap. The residual mass loss of these samples looks similar trend with two steps. The first step was started about 310 ˚C, which correspond to deacetylation in the vinyl acetate, and then the second step is chain scission of the main chain of polyethylene within an interval of 400~500 ˚C (Hoang *et al.*, 2013, Jin *et al.*, 2010, Nyambo *et al.*, 2009).

The thermal degradation for the nanocomposites is shown in Figure 21. The onset temperature of thermal degradation was shifted to higher temperature than pure EVA and the temperature of 50 % residual mass loss ($T_{d50\%}$) was shifted too. These results can be explained that more energy is required to break the bonds which may be attributed to the interfacial interactions between EVA matrix and organoclay which was consistent with the results of the cone calorimeter test (Fang *et al.*, 2009).

As you shown in Table 7, the temperature at 5 % weight loss ($T_{d5\%}$) higher with introduce of organic surfactants. In pure EVA, the $T_{d5\%}$ occurs at 320.1 ˚C while it occurs at from 331.3 to 341.3 ˚C. From these results correspond that thermal degradation retardation is mostly due to a decrease in the rate of evolution of the volatile products (Zanetti *et al.*, 2002). The considerable delay of residual mass loss has been attributed to the barrier effect generated by the dispersed clay which forming an insulating layer. Fluoromica, such as ME with wider platelets than Lap, could act more efficiently as diffusion barriers than shorter Lap type platelets, if the nanocomposites have well dispersion (Peeterbroeck *et al.*, 2005).

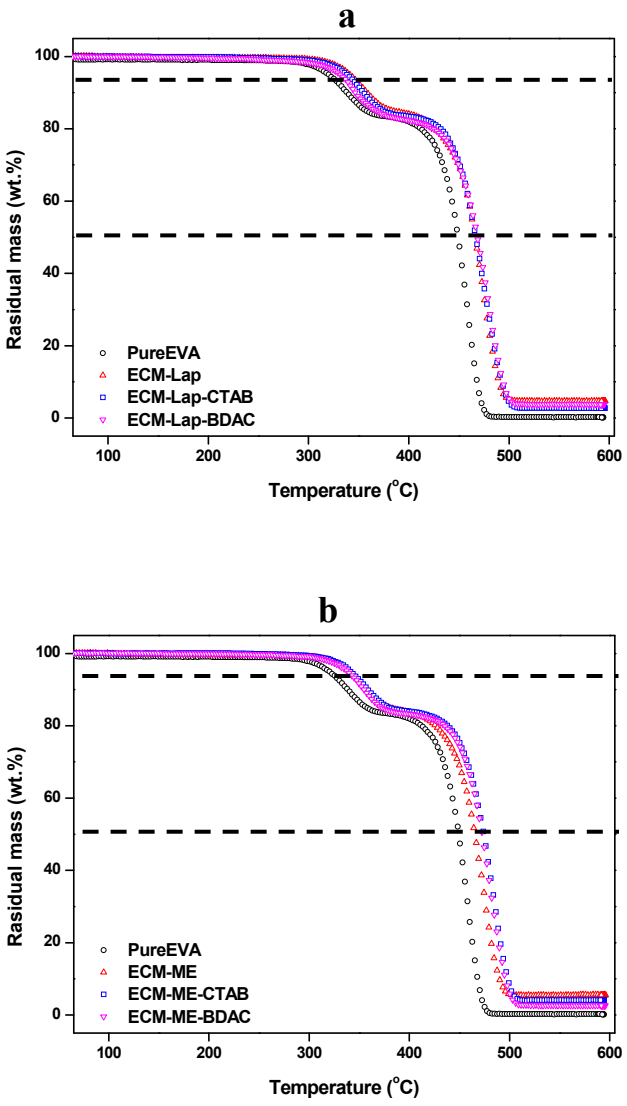

Figure 21. TGA curves of nanocomposites

(A) ECM-Lap series, (b) ECM-ME series

Table 7. TGA data of pure EVA and nanocomposites

	$T_{d5\%}$ (°C)	$T_{d50\%}$ (°C)	Char residue at 600 °C (wt.%)
Pure EVA	320.1	449.3	0
ECM-Lap	340.1	466.4	4.7
ECM-Lap-CTAB	338.1	466.8	2.6
ECM-Lap-BDAC	331.3	468.5	3.7
ECM-ME	340.5	465.3	5.5
ECM-ME-CTAB	341.3	474.1	4.1
ECM-ME-BDAC	338.7	472.6	2.6

4. Conclusion

In this study, the different size pristine clays were modified with different organic surfactants. FT-IR spectroscopy and XRD were used to examine the interaction between alkylammonium and silicate layers. These results proved that the reaction occurred but the degree of reaction was varied depending particle size of clays and kinds of organic surfactants.

And then EVA/clay nanocomposites are fabricated by melt blending. The dispersion of clay in the nanocompositres was investigated using XRD, the composites with organic modified ME shows exfoliated structures, but, the nanocomposites for Lap-series reported intercalated foam and exist of stacked silicate layers. Results obtained from cone calorimeter and TGA indicate that flame retardant and thermal stability and ECM-ME-CTAB and ECM-ME-BDAC showed most efficient behavior. Dispersion of the nanocomposites inside the composites observed from SEM and XRD are better than others, cone calorimeter and TGA results are possibly related to this. Tensile strength, tensile modulus and storage modulus of nanocomposites were increased with ME modified with organic surfactants, while those were not good enough with modified Lap which has smaller particle size. But, there were not significant differences in tensile properties depending on type of organic surfactants.

In this work, nanocomposites with organoclay which possesses particle size of ~1200 nm were showed optimum kind of organoclay inside the composites. There is no significant distinction between CTAB and BDAC, however the nanocomposites fabricated with organic surfactant which has trimethyl quaternary ammonium shows better properties in flame retardant than benzyl dimethyl quaternary ammonium slightly.

Chapter 3

Further Study

1. Introduction

In recent years, various fillers have been introduced to composites. Reinforced fillers are commonly used fillers in the preparation of composite at the micro scale with increase in tensile strength of the composite material sacrificing the elongation at break and discoloring the polymer (Vaia, 2002). So, materials reinforced with nano size materials have been fabricated to overcome this phenomenon. The clays used in the fabrication of polymer nanocomposites are generally of the smectite-type, which have a well-ordered crystalline structure (Sinha Ray and Okamoto, 2003).

In literature, the mechanical properties of some polymers were improved by introducing smectite clay. However, there is critical concentration to lead the best mechanical properties depended on particle size of clays. When polyurethane (PU) nanocomposites were prepared from the unmodified hectorite (HEC), laponite (Lap) and montmorillonite (MMT), HEC-based PU composites was significantly increase by the clay content about 7 wt.% clay, and the tensile strength increased 113.48 %. However, it was not possible to prepare Lap above 5 wt.% because of agglomeration of Lap (Seydibeyoglu *et al.*, 2010). Compared these results, the clays have the most effective level of clay loading.

The aim of this chapter is to investigate critical concentration of mica (ME) modified with cetyltrimethyl ammonium bromide (CTAB) which was shown the best properties in previous research on mechanical properties and combustion behavior.

2. Experimental

2.1. Preparation of EVA/ME-CTAB predispersions

First, the EVA was added to toluene under stirring at 90 ˚C for 1 hour. The dispersion of pristine clay and organoclay in same solvent, prepared by stirring for 6 hours at 90 ˚C, was added to the EVA solution and continuous stirring for 24 hours. A total of the solution was placed in a PET release film and evaporated in oven at 100 ˚C for 12 hours. Table 8 shows the blending ratio of predispersions.

Table 8. Blend ratio of EVA/ME-CTAB predispersions

Samples	ME-CTAB (g)	EVA (g)
ECS-ME-CTAB01	1	4
ECS-ME-CTAB03	3	12
ECS-ME-CTAB05	5	20
ECS-ME-CTAB07	7	28

2.2. Compounding of EVA/ECS-ME-CTAB/MA-g-EVA nanocomposites

EVA was dried at 60 ˚C for 24 hours and stored in polyethylene bags. EVA /ECS series were blended with the MA-g-EVA in a laboratory-sized, co-rotating, twin screw extruder (BA19, Bau Technology, Republic of Korea) using three general processes: melt blending, extrusion and pelletizing. The extruder barrel was divided into eight zones with the temperature in each zone being individually adjustable. The temperature of the mixing zone in the barrel was maintained at 100 ˚C with a screw speed of 300 rpm. The strand after extruding was cooled in a water bath and pelletized with pelletizer (Bau Technology, Republic of Korea). The final pellets were oven dried at 80 ˚C for 24 hours and stored in sealed polyethylene bags to avoid moisture permeation. Table 9 shows the blend ratio of nanocomposites compounded in this work and the manufacturing process of melt blending is same as Chapter 2.2.3, Figure 7.

Table 9. Blend ratio of EVA/ECS-ME-CTAB/MA-g-EVA nanocomposites

Samples	ECS-ME-CTAB series (g)	EVA (wt.%)	MA-g-EVA (wt.%)
Pure EVA	0	100	0
ECM-ME-CTAB01	5	91	5
ECM-ME-CTAB03	15	83	5
ECM-ME-CTAB05	25	75	5
ECM-ME-CTAB07	35	67	5

2.3. Characterization

2.3.1. X-ray diffraction (XRD)

Wide-angle X-ray scattering analysis of pristine clay, organoclay powders and ECM-ME-CTAB nanocomposites were performed using a Bruker X-ray diffractometer (equipped with a 2-D detector) in reflection mode. Tests were carried out with 2θ scanned between 2.0° and 10° nickel-filtered $CuK_{\propto}$ radiation (k = 0.15418 nm) under a voltage of 40 kV and a current of 30 mA.

2.3.2. Cone calorimeter test

Flaming performance was characterized by cone calorimeter (Fire Testing Technology Ltd., UK) according to standard ISO 5660-1. Specimens of 100 mm x 100 mm x 4 mm were irradiated horizontally at a heat flux of 50 kW/m^2.

2.3.3. Tensile test

Tensile tests for the nanocomposites were carried out according to ASTM D 638-03 using a Universal Testing Machine (Zwick Co.) at a crosshead speed of 60 mm/min and a temperature of 23±2 ˚C. Seven measurements were done for each sample and final results were reported as averaged values.

2.3.4. Dynamic mechanical analysis (DMA)

The temperature dependence of the dynamic storage modulus (E') and T_g of nanocomposites was measured at a frequency of 1 Hz and at a strain rate 0.05 % at a heating rate of 2 ˚C/min over the temperature range of -40 ˚C to 40 ˚C. A dynamic mechanical analyzer (DMA Q800, TA Instruments) employing the dual cantilever method in rectangular specimens of 60.0 mm x 12.0 mm x 3.0 mm was used.

2.3.5. Thermal gravimetric analysis (TGA)

TGA measurements were conducted with a thermo gravimetric analyzer (TGA 4000, PerkinElmer Inc., USA) on samples having masses from 5 to 7 mg. The heating rate was 10 ˚C/min over the temperature range from 60 to 600 ˚C; a nitrogen atmosphere was employed.

3. Results and Discussion

3.1. X-ray diffraction (XRD)

Figure 22 shows the evolution of XRD patterns for the nanocomposites with various concentration of ME-CTAB. As you see, there is no peak due to the exfoliation of the silicate in the nanocomposites. It will be talk about this result in cone calorimeter and TGA test, good dispersion is very important in flame retardant and thermal stability. However, there is a slight peak in the nanocomposites with 7 phr of organoclay, indicating the presence both exfoliation and exist of agglomerative particles. This is adversely affected to the thermal degradation and combustion behavior of the nanocomposites. Because, silicate layers in nanocomposites have not enough interaction between EVA matrix, which related its barrier properties in fire (Fang *et al.*, 2009).

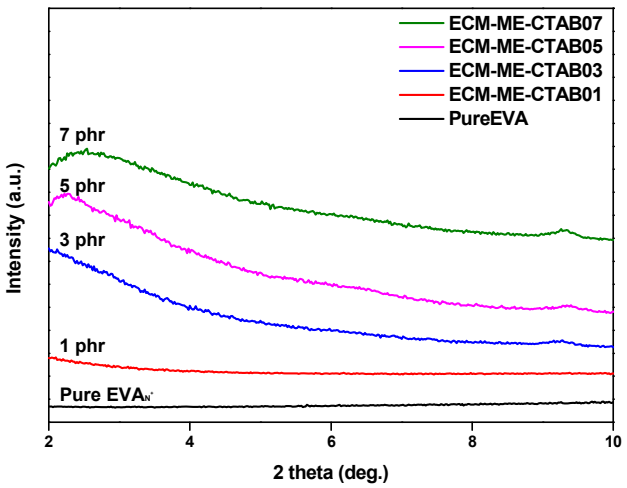

Figure 22. X-ray diffraction patterns of pure EVA and ECM-ME-CTAB series

3.2. Cone calorimeter test

Figure 23 reported the Heat Release Rate (HRR) curves of ECM-ME-CTAB series. The peak Heat Release Rate (pkHRR) was reduced about and the HRR curves became broader with increase in ME-CTAB contents. These results related to the formation of a char layer acted as a blocking and non-burning material, which protected the material against heat flux and reduced the combustion time (Jahromi *et al.*, 2003). However, nanocomposites with over 5 phr of ME-CTAB showed the similar pkHRR and HRR curves. The reduction in pkHRR revealed the flame retardant effect of organoclay, but it is no significant effect more than 5 phr of clay. The pkHRR for the ECM-ME-CTAB05 and ECM-ME-CTAB07 were decreased about 52.5 % and 53.8 % compared with that of the pure EVA respectively. Their pkHRR value 826.1 kW/m^2 and 804.1 kW/m^2 appeared at 240 s and 245 s after the combustion of the specimens in detail. Also, after fire combustion, the char of nanocomposites shows a little different between that ECM-ME-CTAB05 and ECM-ME-CTAB07 (Figure 24). However, none of this result influences its risk of fire.

Figure 25 reported the curve of the Average Rate of Heat Emission (ARHE) and the Maximum Average Rate of Heat Emission (MARHE) is the parameter to determine of the tendency for fire behavior in reality fire circumstance. In previous research, MARHE for the ECM-ME-CTAB05 decreased about 22% compared with that of pure EVA and ECM-ME-CTAB07 showed similar with pkHRR results.

From these data, there was no considerable change in combustion behavior over 5 phr of ME-CTAB in nanocomposites. In previous study by other researchers, they said not only nanocomposites with different dispersion of organoclay displayed different combustion behavior but also there is critical concentration of clay in flame retardant (Beyer, 2001). And

also, the more organoclays added to composites, the more organic matter which can be burned completely.

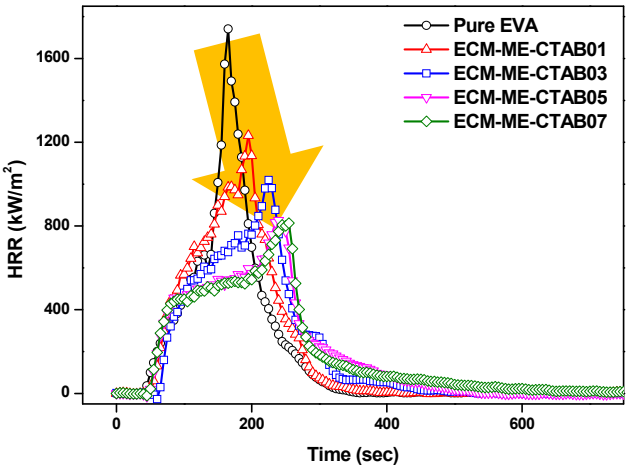

Figure 23. Heat release rate curves of pure EVA and ECM-ME-CTAB series

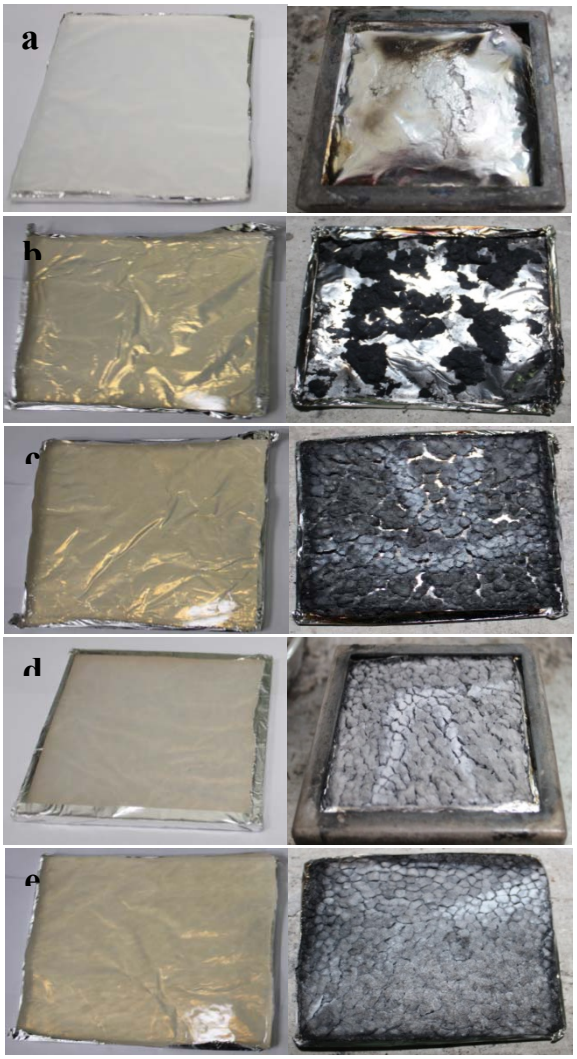

Figure 24. Mass residue after the cone calorimeter tests:
(a) pure EVA, (b) ECM-ME-CTAB01, (c) ECM-ME-CTAB03,
(d) ECM-ME-CTAB05, (e) ECM-ME-CTAB07

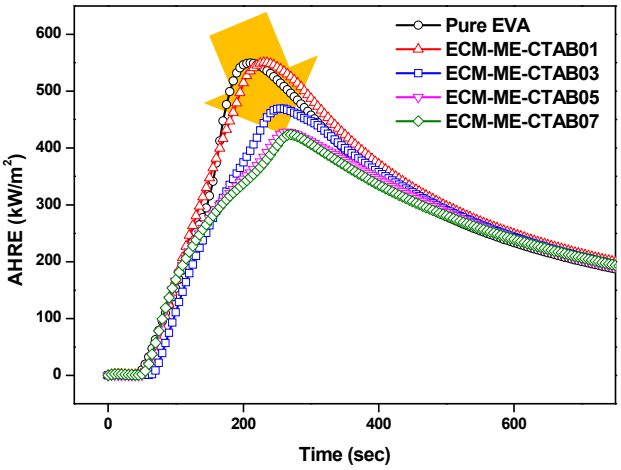

Figure 25. Average rate of heat emission curves of pure EVA and ECM-ME-CTAB series

3.3. Tensile test

Figure 26 shows tensile strength and tensile modulus of nanocomposites obtained from various concentration of ME-CTAB. It is found that the organoclay content has a remarkable effect on the tensile strength and tensile modulus of the nanocomposites. Fortunately, with increasing clay loading, the strength and modulus of nanocomposites increase about 125 % and 233 % respectively, until concentration of organoclay reached optimum level, over 5 phr, in flame retardant. If the excess the clay loading limit presented, tensile properties of nanocomposite declined due to the agglomeration of organoclay particles (Xiong *et al.*, 2004).

Figure 27 shows the relationship between elongation at break and the content of organoclay. As you see, the elongation at break of the nanocomposites decreased with increase of ME-CTAB, and the decrease is slight when organoclay content is above 1 phr. This result is attributed to the interaction between the pure EVA and the silicate layers and the dispersion of organoclay in the EVA matrix (Chang and An, 2002, Ma *et al.*, 2001).

From these results, tensile strength and tensile modulus increased of ME-CTAB. Especially, nanocomposites with the addition of 7 phr organoclay shows the most significant increase. The increased performance is a result of intercalation of nanoclay in composites caused from the interaction between the EVA and silicate layers.

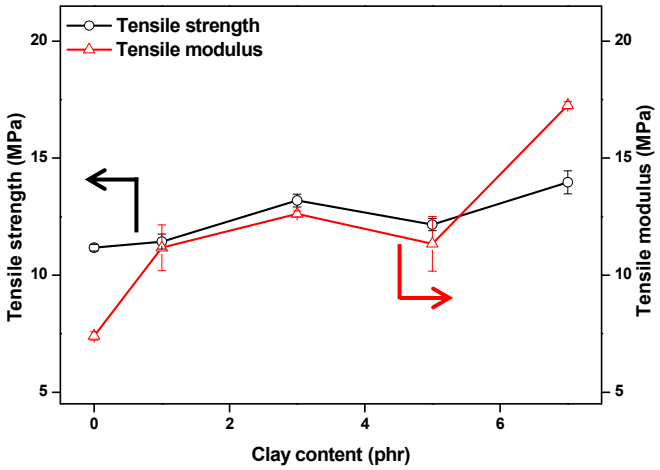

Figure 26. Tensile strength and tensile modulus of pure EVA and ECM-ME-CTAB series

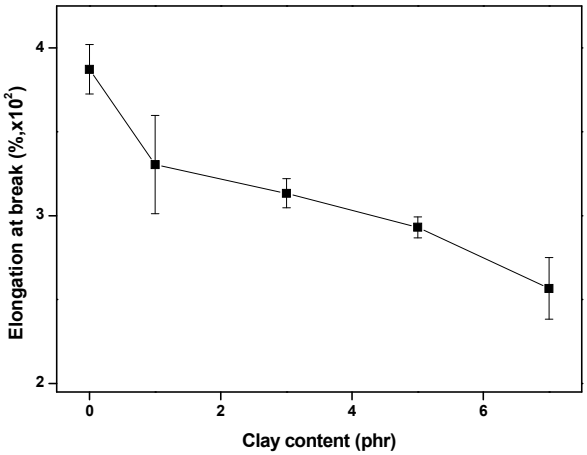

Figure 27. Elongation at break of pure EVA and ECM-ME-CTAB series

3.4. Dynamic mechanical analysis (DMA)

As shown in Figure 28, the variation of the storage modulus with the temperature for nanocomposites. As previous research, the storage modulus of nanocomposites increases with an increase in the organoclay concentration (Vaia *et al.*, 1997, Wu *et al.*, 2002). The enhancement in the storage modulus of the EVA/organoclay nanocomposites is mainly due to the rigid of the clay and the effect of well dispersion. This improvement in the storage modulus with the clay load caused from interaction between silicate layers of clay and EVA matrix (Pramoda and Liu, 2004).

Figure 29 shows the storage modulus at 20 ˚C and the glass transition temperature (T_g) as functions of the clay concentration. The T_g of nanocomposites little increased with an increase in the clay loading. However, it declined rapidly above 5 phr of organoclay. This result is probably due to the plasticizing effect from the presence of organic surfactants in the organoclay (Liu *et al.*, 2003, Pramoda *et al.*, 2003).

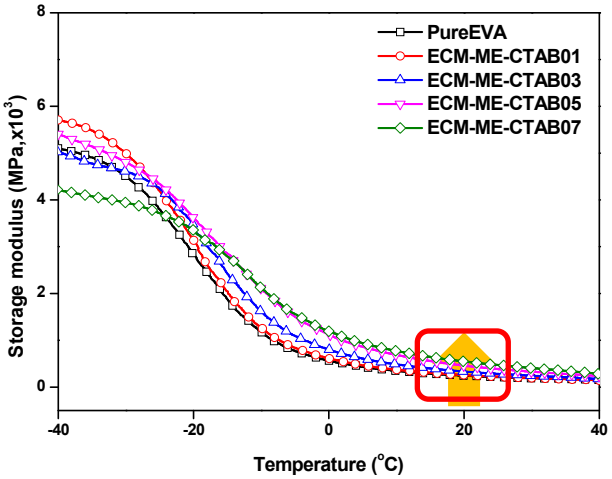

Figure 28. Storage modulus versus temperature plots of pure EVA and ECM-ME-CTAB series

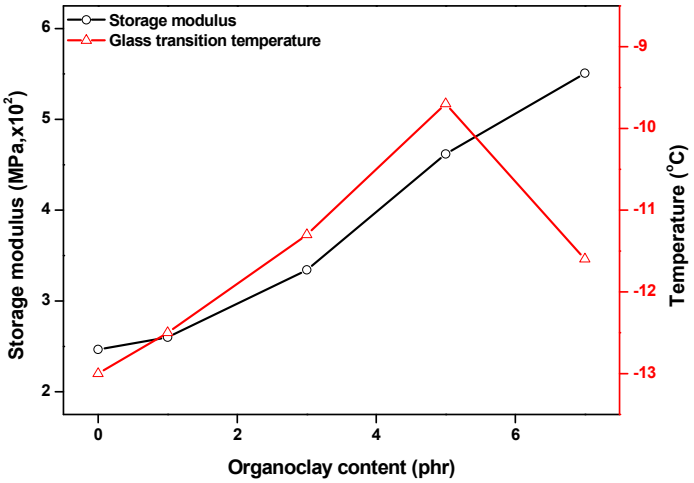

Figure 29. Storage modulus and T_g of pure EVA and ECM-ME-CTAB series

3.5. Thermal gravimetric analysis (TGA)

Figure 30 and Table 9 reports thermal gravimetric curves and data of the composites. The TGA curves of the nanocomposites show two steps of degradation. At first, the deacetylation of vinyl acetate was occurred at about 300 ˚C, and then the main chain of polyethylene was scission within an interval of 400~500 ˚C.

The temperature of 50 % residual mass loss ($T_{d50\%}$) has been indicated parameter for the flame retardants of nanocomposites. As you shown in Table 9, the nanocomposites with 1 and 3 phr of organoclays have little changes with pure EVA and $T_{d50\%}$ of ECM-ME-CTAB05 was increased about 25 ˚C due to the 5 phr of organoclay is enough to generate interaction for barrier effects. On the other hand, $T_{d50\%}$ of ECM-ME-CTAB07 decreased due to too much loading of organoclay which has organic matter which can be burned completely.

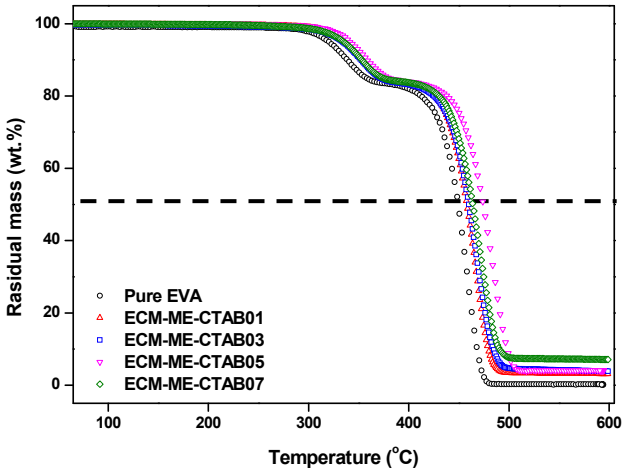

Figure 30. TGA curves of pure EVA and ECM-ME-CTAB series

Table 10. TGA data of pure EVA and nanocomposites

Samples	$T_{d50\%}$ (°C)
Pure EVA	449.3
ECM-ME-CTAB01	458.1
ECM-ME-CTAB03	459.9
ECM-ME-CTAB05	474.1
ECM-ME-CTAB07	463.8

4. Conclusion

In this research, a series of EVA/ME-CTAB/MA-g-EVA nanocomposites with different clay loading was prepared by melt blending. XRD was used to examine the mean spacing between clay silicate layers in nanocomposite. From the XRD diffraction, the nanocomposites with various loading of organoclay show good dispersion which is most important point for properties of composites. Tensile strength, tensile modulus and storage modulus of nanocomposites increase with increase of ME-CTAB loadings. On the other hands, the elongation at break decreased with increase of ME-CTAB, and the decrease is slight above 1 phr of organoclay because of interaction between silicate layers and EVA matrix. The T_g of nanocomposites decreased above the 5 phr of organoclay due to the organic surfactants in nanocomposites act as a plasticizer. The peak heat release rate investigated by a cone calorimeter is drastically reduced. But, there were no significant differences between the nanocomposites with 5 phr and 7 phr of ME-CTAB. In TGA data, the ECM-ME-CTAB07 shows worse thermal degradation properties than ECM-ME-CTAB05. This is due to the present of organic matter which burned in fire completely lead worse thermal properties.

In this work, the nanocomposites show the most outstanding mechanical properties with 7 phr of ME-CTAB. On the other hands, ECM-ME-CTAB05 is sufficient to satisfy the flame retardants. The critical concentration of ME-CTAB in nanocomposites is 5 phr considering both mechanical properties and flame retardants.

References

AKELAH, A. & MOET, A. 1996. Polymer-Clay Nanocomposites: Free-Radical Grafting of Polystyrene on to Organophilic Montmorillonite Interlayers. *Journal of Materials Science,* 31**,** 3589-3596.

ALEXANDRE, M., BEYER, G., HENRIST, C., CLOOTS, R., RULMONT, A. & JØR ME, R. 2001. Preparation and Properties of Layered Silicate Nanocomposites based on Ethylene Vinyl Acetate Copolymers. *Macromolecular Rapid Commuications,* 22**,** 643-646.

ASYADI, F., JAWAID, M., HASSAN, A. & WAHIT, M. U. 2013. Mechanical Properties of Mica-Filled Polycarbonate/Poly(Acrylonitrile-Butadiene-Styrene) Composites. *Polymer-Plastics Technology and Engineering,* 52**,** 727-736.

BEYER, G. N. 2001. Flame Retardant Properties of EVA-Nanocomposites and Improvements by Combination of Nanofillers with Aluminium Trihydrate. *Fire and Materials,* 25**,** 193-197.

BIGG, D. M. 1987. Mechanical Properties of Particulate filled Polymers. *Polymer Composite,* 8**,** 115-122.

BOYD, S. A., SHAOBAI, S., LEE, J.-F. & MORTLAND, M. M. 1988. Pentachlorophenol Sorption by Organo-Clays. *Clays and Clay Minerals,* 36**,** 125.

CAO, J.-P., ZHAO, X., ZHAO, J., HU, G.-H. & DANG, Z.-M. 2013. Improved Thermal Conductivity and Flame Retardancy in Polystyrene/Poly(Vinylidene Fluoride) Blends by Controlling Selective Localization and Surface Modification of SiC Nanoparticles. *Applied Materials & Interfaces,* 5**,** 6915-6924.

CHANG, J.-H. & AN, Y. U. 2002. Nanocomposites of Polyurethan with various Organoclys: Thermomechanical Properties, Morphology, and Gas Permeability. *Journal of Polymer Science Part B: Polymer Physics,* 40**,** 670-677.

CHAO, H. & RIGGLEMAN, R. A. 2013. Effect of Particle Size and Grafting Density on the Mechanical Properties of Polymer Nanocomposites. *Polymer,* 54**,** 5222-5229.

DIKOBE, D. G. & LUYT, A. S. 2010. Morphology and Thermal Properties of Maleic Anhydride Grafted Polyprolylene/Ethylene-Vinyl Acetate Copolymer/Wood Powder Blend Composites. *Journal of Applied Polymer Science,* 116**,** 3193-3201.

DUGGAN, G., GRAYSON, S. & KUMAR, S. 2004. New Fire Classifications and Fire Test Methods for the European Railway Industry. *In: Proceedings flame retardants, London: Interscience Communications*.

FANG, S., HU, Y., SONG, L. & WU, J. 2009. Preparation and Investigation of Ethylene–Vinyl Acetate Copolymer/Silicone Rubber/Clay Nanocomposites. *Journal of Applied Polymer Science,* 113**,** 1664-

1670.
FINA, A., ABBENHUIS, H. C. L., TABUANI, D. & CAMINO, G. 2006. Metal Functionalized POSS as Fire Retardants in Polypropylene. *Polymer Degradation and Stability,* 91**,** 2275-2281.
FOUNGFUNG, D., PHATTANARUDEE, S., SEETAPANC, N. & KIATKAMJORNWONG, S. 2011. Acrylamide–Itaconic Acid Superabsorbent Polymers and Superabsorbent Polymer/Mica Nanocomposites. *Polymer for Advanced Technologies,* 22**,** 635-647.
GINZBURG, V. V., SINGH, C. & BALAZS, A. C. 2000. Theoretical Phase Diagrams of Polymer/Clay Composites: The Role of Grafted Organic Modifiers. *Macromolecules*, 33, 1089-1099.
HASEGAWA, N., OKAMOTO, H., KAWASUMI, M., KATO, M., TSUKIGASE, A. & USUKI, A. 2000. Polyolefin-Clay Hybrids based on modified Polyolefins and Organophilic Clay. *Macromolecular Materials and Engineering,* 280/281**,** 76-79.
HOANG, T., CHINH, N. T., TRANG, N. T. T., HANG, T. T. X., THANH, D. T. M., HUNG, D. V., HA, C.-S. & AUFRAY, M. 2013. Effects of Maleic Anhydride grafted Ethylene/Vinyl Acetate Copolymer (EVA) on the Properties of EVA/Silica Nanocomposites. *Macromolecular Research,* 21**,** 1210-1217.
JAHROMI, S., GABRIE¨LSE, W. & BRAAM, A. 2003. Effect of Melamine Polyphosphate on Thermal Degradation of Polyamides: a combined X-ray Diffraction and Solid-State NMR Study. *Polymer,* 44**,** 25-37.
JIN, J., CHEN, S. & ZHANG, J. 2010. UV Aging Behaviour of Ethylene-Vinyl Acetate Copolymers (EVA) with different Vinyl Acetate Contents. *Polymer Degradation and Stability,* 95**,** 725-732.
KEENER, T. J., STUART, R. K. & BROWN, T. K. 2004. Maleated Coupling Agents for Natural Fibre Composite. *Composites: Part A Applied Science and Manufacturing,* 35**,** 357-362.
KHAN, M. A. & BHATTACHARIA, S. K. 2007. Effect of Novel Coupling Agent on the Mechanical and Thermal Properties of Unidirectional Jute–Vinyl Ester Composites. *Journal of Reinforced Plastics and Composites,* 26**,** 617-627.
LEE, K. M. & HAN, C. D. 2003a. Effect of Hydrogen Bonding on the Rheology of Polycarbonate/Organoclay Nanocomposites. *Polymer,* 44**,** 4573-4588.
LEE, K. M. & HAN, C. D. 2003b. Rheology of Organoclay Nanocomposites: Effects of Polymer Matrix/Organoclay Compatibility and the Gallery Distance of Organoclay. *Macromolecules,* 36**,** 7165-7178.
LIMPARYOON, N., SEETAPAN, N. & KIATKAMJORNWONG, S. 2011. Acrylamide/2-Acrylamido-2-Methylpropane Sulfonic Acid and

associated Sodium Salt Superabsorbent Copolymer Nanocomposites with Mica as Fire Retardants. *Polymer Degradation and Stability,* 96**,** 1054-1063.

LIU, T., LIM, K. P., TJIU, W. C., PRAMODA, K. P. & CHEN, Z.-K. 2003. Preparation and Characterization of Nylon 11/Organoclay Nanocomposites. *Polymer,* 44**,** 3529-3535.

MA, J., ZHANG, S. & QI, Z. 2001. Synthesis and Characterization of Elastomerix Polyurethane/Clay Nanocomposites. *Journal of Applied Polymer Science,* 82**,** 1444-1448.

MADEJOVA´, J., BUJDA´K, J., JANEK, M. & KOMADEL, P. 1998. Comparative FT-IR Study of Structural Modifications during Acid Treatment of Dioctahedral Smectites and Hectorite. *Spectrochimica Acta Part A,* 54**,** 1397-1406.

MICHOT, L. J. & PINNAVAIA, T. J. 1991. Adsorption of Chlorinated Phenols from Aqueous Solution by Surfactant-Modified Pillared Clays. *Clays and Clay Minerals,* 39**,** 634-641.

MITTAL, V. 2009. Polymer Layered Silicate Nanocomposites: A Review. *Materials,* 2**,** 992-1057.

MONTI, M. & CAMINO, G. 2013. Thermal and Combustion Behavior of Polyethersulfone-Boehmite Nanocomposites. *Polymer Degradation and Stability,* 98**,** 1838-1846.

NAFFAKH, M., DIEZ-PASCUAL, M., MARCO, C., GOMEZ, M. A. & JIMENEZ, I. 2010. Novel Melt-Processable Poly(ether ether ketone)(PEEK)/Inorganic Fullerene-like WS_2 Nanoparticles for Critical Applications. *The Journal of Physical Chemistry B,* 114**,** 11444-11453.

NUGAY, N. & ERMAN, B. 2001. Property Optimization in Nitrule Rubber Composites via Hybrid Filler Systems. *Journal of Applied Polymer Science,* 79**,** 366-374.

NYAMBO, C., KANDARE, E. & WILKIE, C. A. 2009. Thermal Stability and Flammability Characteristics of Ethylene Vinyl Acetate (EVA) Composites blended with a Phenyl Phosphonate-Intercalated Layered Double Hydroxide (LDH), Melamine Polyphosphate and/or Boric Acid. *Polymer Degradation and Stability,* 94**,** 513-520.

OSMAN, M. A., RUPP, J. E. & SUTER, U. W. 2005. Gas Permeation Properties of Polyethylene-Layered Silicate Nanocomposites. *Journal of Materials Chemistry,* 15**,** 1298-1304.

OZMIHCI, F. O. & BALKOSE, D. 2013. Effects of Particle Size and Electrical Resistivity of Filler on Mechanical, Electrical, and Thermal Properties of Linear Low Density Polyethylene-Zinc Oxide Composites. *Journal of Applied Polymer Science,* 130**,** 2734-2743.

PARK, Y. J., JOO, H. S., KIM, H. J. & LEE, Y. K. 2006. Adhesion and Rheological Properties of EVA-based Hot-Melt Adhesives. *International Journal of Adhesion & Adhesives,* 26**,** 571-576.

PAVLACKY, E. & WEBSTER, D. C. 2012. Polymer/Clay Nanocomposite Plasticization: Elucidating the Influence of Quaternary Alkylammonium Organic Modifiers. *Journal of Applied Polymer Science,* 129**,** 324-333.

PAVLIDOUA, S. & PAPASPYRIDESB, C. D. 2008. A Review on Polymer–Layered Silicate Nanocomposites. *Progress in Polymer Science,* 33**,** 1119-1198.

PEETERBROECK, S., ALEXANDRE, M., JE´RO^ME, R. & DUBOIS, P. 2005. Poly(ethylene-co-vinyl acetate)/Clay Nanocomposites: Effect of Clay Nature and Organic Modifiers on Morphology, Mechanical and Thermal Properties. *Polymer Degradation and Stability,* 90**,** 288-294.

PORTER, D., METCALFE, E. & THOMAS, J. K. 2000. Nanocomposite Fire Retardants - A Review. *Fire and Materials,* 24**,** 45-52.

PRAMODA, K. P. & LIU, T. 2004. Effect of Moisture on the Dynamic Mechanical Relaxation of Polyamide-6/Clay Nanocomposites. *Journal of Polymer Science Part B: Polymer Physics,* 42**,** 1823-1830.

PRAMODA, K. P., LIU, T., LIU, Z., HEA, C. & SUE, H.-J. 2003. Thermal Degradation Behavior of Polyamide 6/Clay Nanocomposites. *Polymer Degradation and Stability,* 81**,** 47-56.

PREMALAL, H. G. B., ISMAIL, H. & BAHARIN, A. 2002. Comparison of the Mechanical Properties of Rice Husk Powder filled Polypropylene Composites with Talc filled Polypropylene Composites. *Polymer Testing,* 21**,** 833-839.

RIVA, A., ZANETTI, M., BRAGLIA, M., CAMINO, G. & FALQUIC, L. 2002. Thermal Degradation and Rheological Behaviour of EVA/Montmorillonite Nanocomposites. *Polymer Degradation and Stability,* 77**,** 299-304.

SEYDIBEYOGLU, M. O., ISCI, S., GUNGOR, N., ECE, O. I. & GUNER, F. S. 2010. Preparation of Polyurethane/Hectorite, Polyurethane/Montmorillonite, and Polyurethane/Laponite Nanocomposites without Organic Modifiers. *Journal of Applied Polymer Science,* 116**,** 832-837.

SHI, Y., PETERSON, S. & SOGAH, D. Y. 2007. Surfactant-Free Method for the Synthesis of Poly(vinyl acetate) Masterbatch Nanocomposites as a Route to Ethylene Vinyl Acetate/Silicate Nanocomposites. *Chemistry of Materials,* 19**,** 1552-1564.

SIENGCHIN, S. & KARGER-KOCSIS, J. 2009. Structure and Creep Response of toughened and nanoreinforced Polyamides produced

via the Latex Route: Effect of Nanofiller Type. *Composites Science and Technology,* 69**,** 677-683.

SINHA RAY, S. & OKAMOTO, M. 2003. Polymer/Layered Silicate Nanocomposites: A Review from Preparation to Processing. *Progress in Polymer Science,* 28**,** 1539-1641.

SOUZA, D. H. S., DAHMOUCHE, K., ANDRADE, C. T. & DIAS, M. L. 2011. Structure, Morphology and Thermal Stability of Synthetic Fluorine Mica and its Organic Derivatives. *Applied Clay Science,* 54**,** 226-234.

SUH, I. S., RYU, S. H., BAE, J. H. & CHANG, Y. W. 2004. Effects of Compatibilizer on the Layered Silicate/ Ethylene Vinyl Acetate Nanocomposite. *Journal of Applied Polymer Science,* 94**,** 1057-1061.

THIRMIZIR, M. Z. A., ISHAK, Z. A. M., TAIB, R. M., RAHIM, S. & JANI, S. M. 2011. Kenaf-Bast-Fiber-Filled Biodegradable Poly(butylene succinate) Composites: Effects of Fiber Loading, Fiber Length, and Maleated Poly(butylene succinate) on the Flexural and Impact Properties. *Journal of Applied Polymer Science,* 122**,** 3055-3063.

VAIA, R. 2002. Polymer Nanocomposites Open a New Dimension for Plastics and Composites. *AMPTIAC Newsletter,* 6**,** 17-24.

VAIA, R. A., SAUER, B. B., TSE, O. K. & GIANNELIS, E. P. 1997. Relaxations of Confined Chains in Polymer Nanocomposites: Glass Transition Properties of Poly (ethylene oxide) intercalated in Montmorillonite. *Journal of Polymer Science Part B: Polymer Physics,* 35**,** 59-67.

WANG, L., ZHAO, X., CHEN, C. & CAO, J. 2012. Effect of Rare Earth Ions on the Properties of Composites Composed of Ethylene Vinyl Acetate Copolymer and Layered Double Hydroxides. *Effect of Rare Earth Ions on the Composites,* 7**,** 1-11.

WU, Q., ZHU, W., ZHANG, C., LIANG, Z. & WANG, B. 2010. Study of Fire Retardant Behavior of Carbon Nanotube Membranes and Carbon Nanofiber Paper in Carbon Fiber Reinforced Epoxy Composites. *Carbon,* 48.

WU, Z., ZHOU, C., QI, R. & ZHANG, H. 2002. Synthesis and Characterization of Nylon 1012/Clay Nanocomposite. *Journal of Applied Polymer Science,* 83**,** 2403-2410.

XI, Y., DING, Z., HE, H. & FROST, R. L. 2004. Structure of Organoclays—an X-ray Diffraction and Thermogravimetric Analysis Study. *Journal of Colloid and Interface Science,* 277**,** 116-120.

XIONG, J., LIU, Y., YANG, X. & WANG, X. 2004. Thermal and Mechanical Properties of Polyurethane/Montmorillonite

Nanocomposites based on a novel reactive Modifier *Polymer Degradation and Stability,* 86**,** 549-555.

YANG, H.-S., KIM, H.-J., PARK, H.-J., LEE, B.-J. & HWANG, T.-S. 2007. Effect of Compatibilizing Agents on Rice-Husk Flour reinforced Polypropylene Composites. *Composite Structures,* 77**,** 45-55.

YANG, J.-H., HAN, Y.-S., CHOY, J.-H. & TATEYAMA, H. 2001. Intercalation of Alkylammonium Cations into expandable Fluorine Mica and its Application for the Evaluation of heterogeneous Charge Distribution. *Journal of Materials Chemistry,* 11**,** 1305-1312.

YANG, J., FAN, H., BU, Z. & LI, B.-G. 2009. Influence of Clay and Predispersion Method on the Structure and Properties of Polystyrene(PS)-Clay Nanocomposites. *Polymer Engineering and Science,* 49**,** 1937-1944.

YANG, J., SUN, L., XIANG, S., HE, J., GU, L. & ZHONG, M. 2008. Influence of Organoclay and Preparation Technique on the Morphology of Polyamide6/Polystyrene/Organoclay Nanocomposites. *Journal of Applied Polymer Science,* 110**,** 276-282.

ZANETTI, M., KASHIWAGI, T., FALQUI, L. & CAMINO, G. 2002. Cone Calorimeter Combustion and Gasification Studies of Polymer Layered Silicate Nanocomposites. *Chemistry of Materials,* 14**,** 881-887.

ZHU, J., WANG, T., ZHU, R., GE, F., WEI, J., YUAN, P. & HE, H. 2011. Novel Polymer/Surfactant modified Montmorillonite Hybrids and the Implications for the Treatment of Hydrophobic Organic Compounds in Wastewaters. *Applied Clay Science,* 51**,** 317-322.

초 록

나노복합재료는 일반적인 마이크로- 및 마크로- 복합재료에 비하여 산업 및 학계에 큰 관심을 받고 있다. 특히, 층상 구조를 갖는 양이온성 클레이는 소량만으로도 고분자의 성능을 향상시킴과 동시에 소재의 경량화를 만족시킬 수 있다. 에틸렌 비닐 아세테이트 (ethylene vinyl acetate; EVA)는 와이어, 케이블, 포장지 및 접착제 산업에 널리 이용되고 있다. 경제성이 높고 비교적 우수한 전기적 성질(electrical property) 및 베리어 성능(barrier property)을 가짐으로 시장에서 그 관심은 지속적으로 증가하고 있다. 하지만, 인장강도 및 열 안정성이 떨어짐으로써 몇몇 분야로의 적용이 제한되고 있다. 최근 이와 같은 장애를 극복하기 위해 고분자에 나노 파티클을 적용하려는 연구가 활발히 진행되고 있다.

본 연구에서는 파티클 사이즈가 다른 양이온성 클레이(Mica; ~1200 nm, Laponite; ~25 nm) 및 고분자와의 혼화성을 높이기 위한 두 종류의 유기 계면 활성제(ctyltrimetylammonium bromide; CTAB, bezyldimetylstearylammonium chloride; BDAC)를 선택하여 기계적 강도, 열 안정성 및 난연성이 개선된 에틸렌 비닐 아세테이트-양이온성 클레이 나노복합재료를 제작하였으며 이 중 가장 탁월한 유기화 클레이의 농도를 달리하여 복합재료의 성능을 평가하였다.

유기화 클레이의 유기화 유무를 확인하기 위해 FT-IR 및 XRD 측정을 통하여 확인하였다. FT-IR을 통해 클레이내의 tetrahedral sheet에 존재하는 Si-O의 구조적 변화와 유기화로 인

한 알킬기의 삽입을 확인하였으며 XRD를 통해 실리케이트층간 거리의 변화를 통해 유기화를 확인하였다.

Cone calorimeter를 통해 연소 거동을 관찰하였을 때, 화재발생 시 위협이 되는 최대발열량에 있어 순수한 EVA와 비교하였을 때 CTAB로 유기화 처리한 Mica (ME-CTAB)의 경우 52 % 저감률을 나타내었다. 실제 크기의 조건에서 화재 발생 경향을 확인할 수 있는 파라미터로 이용되어 온 Maximum Average Rate of Heat Emission (MARHE)는 22% 저감되어 마찬가지로 탁월한 난연성을 확인하였다. 또한, ME-CTAB의 함량이 증가할수록 난연성 또한 향상되었지만 5 phr 이상에서는 비슷한 경향을 보였다. 반면, Mica에 비하여 파티클 사이즈가 작은 Laponite의 경우 내표면적이 증가함으로써 균일한 분산을 만족시키지 못하고 클레이의 실리케이트 층 내부에 유기제의 존재로 인하여 난연성에 있어 순수한 클레이보다 오히려 저하되었다.

복합재료의 인장성질 및 점탄성적 특성을 측정하였을 때, 필러의 첨가로 인하여 향상되었고 고분자와의 혼화성이 향상된 유기화 클레이의 경우 보다 더 향상되었다. 하지만 분산성에 문제를 갖는 Laponite를 사용한 복합재료는 전체적으로 그 성질이 저하되었다. 마찬가지로 ME-CTAB의 함량이 증가할수록 인장강도, 인장탄성률 및 저장탄성율은 증가하였으나 매트릭스와 실리케이트층과의 결합이 강해짐으로써 신장률은 저하되었고 5 phr 이상의 유기화 클레이가 첨가되었을 때, 클레이내의 유기 계면활성제로 인한 가소화 효과로 인하여 복합재료의 T_g는 약간 저하되었다.

복합재의 파단면을 관찰하기 위해 SEM을 측정하였다. 부분적으로 응집체를 확인할 수 있었으나 Mica의 경우 유기화될수

록 응집체의 크기가 작아졌으나 Laponite의 경우 유기화시 오히려 응집체의 크기가 커짐을 확인할 수 있었다. 이는 고분자와의 혼화성을 위해 처리한 유기화가 오히려 클레이간의 응집을 촉진시켰음을 알 수 있었다. 또한, 이 결과는 인장실험 시 인장탄성률 및 저장탄성율의 결과를 설명해 줄 수 있었다.

복합재료의 열안정성 및 난연성을 예측하기 위하여 TGA를 측정하였다. 열안정성과 난연성은 질량감소율이 각각 5%, 50%에 달했을 때의 온도를 비교하여 관찰할 수 있다. 순수한 EVA ($T_{d5\%}$=320.1℃, $T_{d50\%}$=449.3℃)에 비하여 ME-CTAB를 이용한 나노복합재료 ($T_{d5\%}$=341.3℃, $T_{d50\%}$=474.1℃)의 열안정성 및 난연성이 향상되었다. Laponite를 이용한 복합재료 또한 전체적으로 향상되었으나 분산성의 한계로 인하여 mica를 이용한 것에 비해 낮으며 순수한 양이온성 클레이와 유기화 클레이의 경우 큰 차이를 보이지 않았다. 난연성에 있어 ME-CTAB의 함량이 증가할 시 1, 3 (phr)를 첨가하였을 때에는 순수한 EVA에 비하여 큰 차이를 보이지 않으나 5 phr를 첨가하면 약 25 ℃ 향상되는 반면, 이상의 량이 첨가되면 유기화 클레이내의 유기체의 량이 과하여 다시 저하되었다.

키워드 : 나노복합재료, 에틸렌 비닐 아세테이트, 유기화 클레이, 기계적 물성, 난연성

학번 : 2012-21119